

Supplementary Information

Approaches to selective fibroblast growth factor receptor 4 inhibition through targeting the ATP-pocket middle-hinge region

Robin A. Fairhurst*, Thomas Knoepfel, Catherine Leblanc, Nicole Buschmann, Christoph Gaul, Jutta Blank, Inga Galuba, Jörg Trappe, Chao Zou, Johannes Voshol, Christine Genick, Peggy Brunet-Lefevre, Francis Bitsch, Diana Graus-Porta, Pascal Furet

Novartis Institutes for BioMedical Research, CH-4002 Basel, Switzerland.

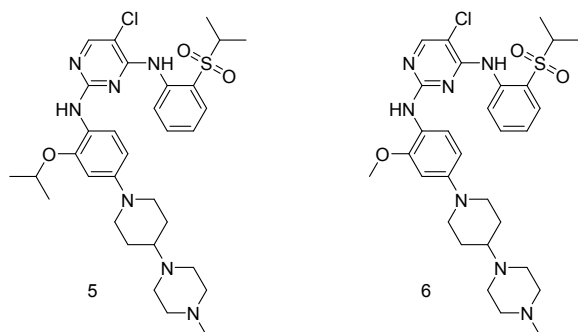
Table of contents	Page
1 Compound synthesis	2
2 NMR spectra	10
3 Molecular modeling	15
4 Biochemical FGFR assays	19
5 Selected profiling data for compound 7	24
6 FGFR4 mass spectroscopy studies	26
7 FGFR4 X-ray structure determinations	30
8 Determination of the FGFR4 resynthesis rates	32
9 X-Ray structure determination for compound 10	34
10 References	35

1 Compound synthesis

Experimental Procedures

Solvents and reagents were purchased from suppliers and used without any further purification. Normal phase chromatography was conducted using a Teledyne ISCO, CombiFlash Rf system with silica gel pre-packed columns (RediSep® Rf) and TLC plates pre-coated with silica gel 60 F 254 on aluminum (Merck KGaA) with detection by UV (254 nm). The pH of solutions were measured using pHix 0-14 paper (FisherBrand). LC/MS was conducted using: Waters Acquity UPLC with Waters SQ detector; with a Acquity HSS T3 1.8 μ m 2.1 x 50 mm column; eluting with gradients of aqueous acetonitrile containing formic acid and ammonium acetate modifiers. Proton, fluorine and carbon NMR experiments were performed using Bruker Ultrashield 400, Varian Mercury 400 MHz and 500 MHz DRX Bruker CryoProbe instruments. Chemical shifts (δ) are quoted in ppm relative to residual proton peaks in solvent. The multiplicity of the signals are indicated as s-singlet, d-doublet, t-triplet, q-quartet, p-pentet, hept-heptet, m-multiplet, or br-broad. Coupling constants are quoted in Hz to one decimal place. For NMR, the solvents were chosen according to the position of solvent peaks in the spectra and based upon the solubility of the measured compound. Within this text, room temperature (RT) is defined as 19 – 25 °C. The term in vacuo is used to describe solvent removal by Büchi rotary evaporation between 17 and 40 °C, at 20 - 500 mbar unless otherwise stated.

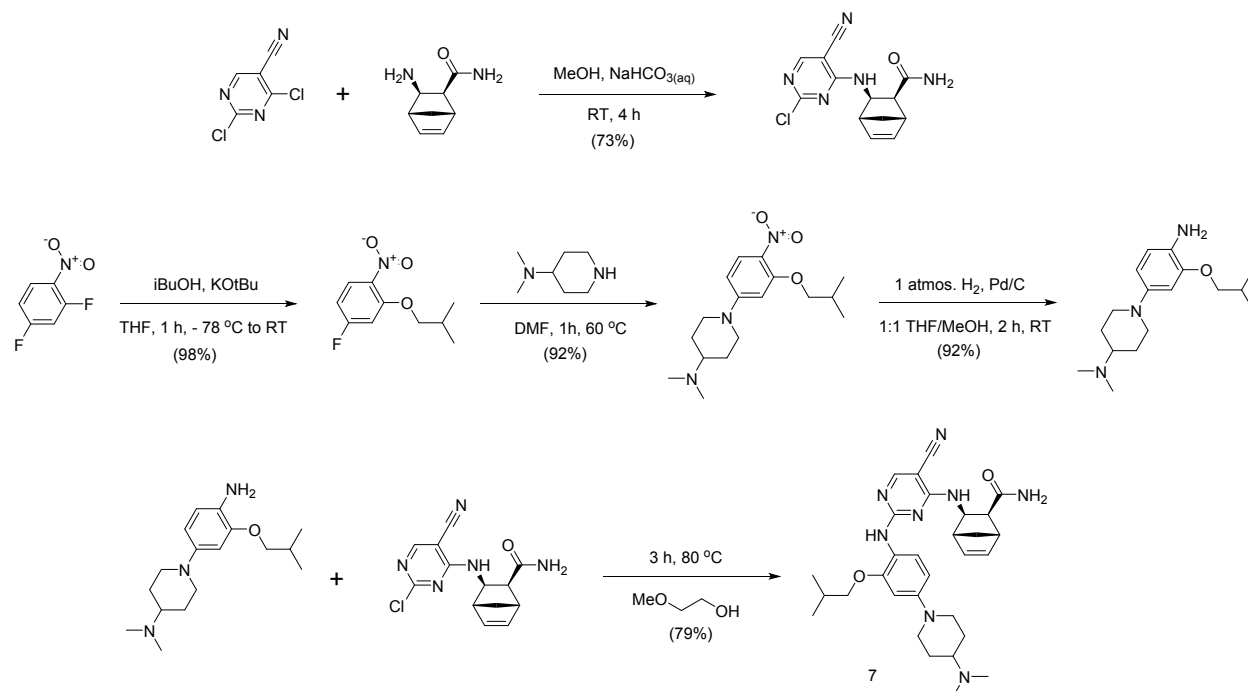
Compounds 5 and 6 were prepared as described in reference 22 in the main text.



5-Chloro-*N*²-(2-isopropoxy-4-(4-(4-methylpiperazin-1-yl)piperidin-1-yl)phenyl)phenyl)-*N*⁴-(2-(isopropylsulfonyl)phenyl)pyrimidine-2,4-diamine 5: off-white solid, ¹H NMR (400 MHz, DMSO-*d*₆) δ 9.50 (s, 1H), 8.52 (br, d, *J* = 8.5 Hz, 1H), 8.17 (s, 1H), 8.09 (s, 1H), 7.78 (dd, *J* = 8.0, 1.5 Hz, 1H), 7.55 (br, t, *J* = 7.9 Hz, 1H), 7.38 (d, *J* = 8.7 Hz, 1H), 7.29 (t, *J* = 7.6 Hz, 1H), 6.59 (s, 1H), 6.45 (dd, *J* = 8.8, 2.4 Hz, 1H), 4.55 (hept, *J* = 6.1 Hz, 1H), 3.73 – 3.60 (m, 2H), 3.40 (p, *J* = 6.8 Hz, 1H), 3.35 – 3.23 (m, 4H), 2.69 – 2.57 (m, 2H), 2.42 – 2.19 (m, 5H), 2.13 (s, 3H), 1.82 (br, d, *J* = 12.2 Hz, 2H), 1.49 (br, qd, *J* = 12.0, 3.7 Hz, 2H), 1.15 (m, 12H).

5-Chloro-*N*⁴-(2-(isopropylsulfonyl)phenyl)phenyl)-*N*²-(2-methoxy-4-(4-(4-methylpiperazin-1-yl)piperidin-1-yl)phenyl)pyrimidine-2,4-diamine 6: off-white solid, ¹H NMR (400 MHz, acetic acid-*d*₄) δ 8.45 (d, *J* = 8.3 Hz, 1H), 8.21 (s, 1H), 8.00 – 7.88 (m, 2H), 7.70 (t, *J* = 7.8 Hz, 1H), 7.41 (t, *J* = 7.6 Hz, 1H), 7.29 (s, 1H), 7.12 (d, *J* = 9.1 Hz, 1H), 4.11 – 3.70 (m, 14H), 3.49 – 3.39 (m, 2H), 3.30 (p, *J* = 6.8 Hz, 1H), 3.01 (s, 3H), 2.52 (br,s, 4H), 1.25 (d, *J* = 6.8 Hz, 6H).

Compound 7 was prepared as outlined below.



Step 1: (1S,2S,3R,4R)-3-(2-chloro-5-cyanopyrimidin-4-ylamino)bicyclo[2.2.1]hept-5-ene-2-carboxamide. (1S,2S,3R,4R)-3-aminobicyclo[2.2.1]hept-5-ene-2-carboxamide trifluoroacetate (1.4 g, 5.26 mmol)^{S1} was added portion wise to a solution of 2,4-dichloro-5-cyanopyrimidine (0.94 g, 5.26 mmol) and sodium bicarbonate (1.33 g, 15.8 mmol) in methanol (15 ml) and water (15 ml), cooled with an ice bath. After stirring 4 h the reaction mixture is partitioned between CH₂Cl₂ and water, extracted a further 2x with CH₂Cl₂, the combined organic extracts are dried over sodium sulfate and evaporated. The crude product was purified by normal phase chromatography, eluting with a gradient from CH₂Cl₂ to 40% EtOAc in CH₂Cl₂, to give the desired product as the higher running predominant peak, as a white solid, weight = (1.1 g, 73% yield). The regioisomeric (1S,2S,3R,4R)-3-(4-chloro-5-cyanopyrimidin-2-ylamino)bicyclo[2.2.1]hept-5-ene-2-carboxamide eluted directly after, as a white solid, weight = (0.3 g, 15% yield). ¹H NMR (400 MHz, CDCl₃) δ 8.51 (br, s, 1H), 8.25 (s, 1H), 6.42 – 6.17 (m, 3H), 5.75 (br, m, 1H), 4.27 (dd, *J* = 8.7, 6.8 Hz, 1H), 3.06 (s, 1H), 2.87 (s, 1H), 2.45 (d, *J* = 7.7 Hz, 1H), 2.17 (d, *J* = 9.4 Hz, 1H), 1.61 (d, *J* = 9.4 Hz, 1H).

Step 2: 4-fluoro-2-isobutoxy-1-nitrobenzene. A solution of isobutanol (5.80 ml, 62.9 mmol) in THF (100 ml) under argon was cooled in an ice bath and treated portion wise with potassium tert.butoxide (9.17 g, 82 mmol). After complete addition the bath was removed and the reaction mixture was stirred for 30 min. The reaction mixture was cooled to -78 °C and then 2,4-difluoronitrobenzene (6.89 ml, 62.9 mmol) was added via syringe at such a rate that the internal temperature did not exceed -65 °C. After complete addition the dark brown reaction mixture was stirred 5 min and then the cooling bath was removed and the reaction mixture was stirred for 1 h. The reaction mixture was poured into water, extracted 2x with EtOAc. The combined organic layers were washed with brine, dried over anhydrous Na₂SO₄, filtered and concentrated under reduced pressure to give the desired product as red oil (13.08 g, 61.3 mmol, 98 %

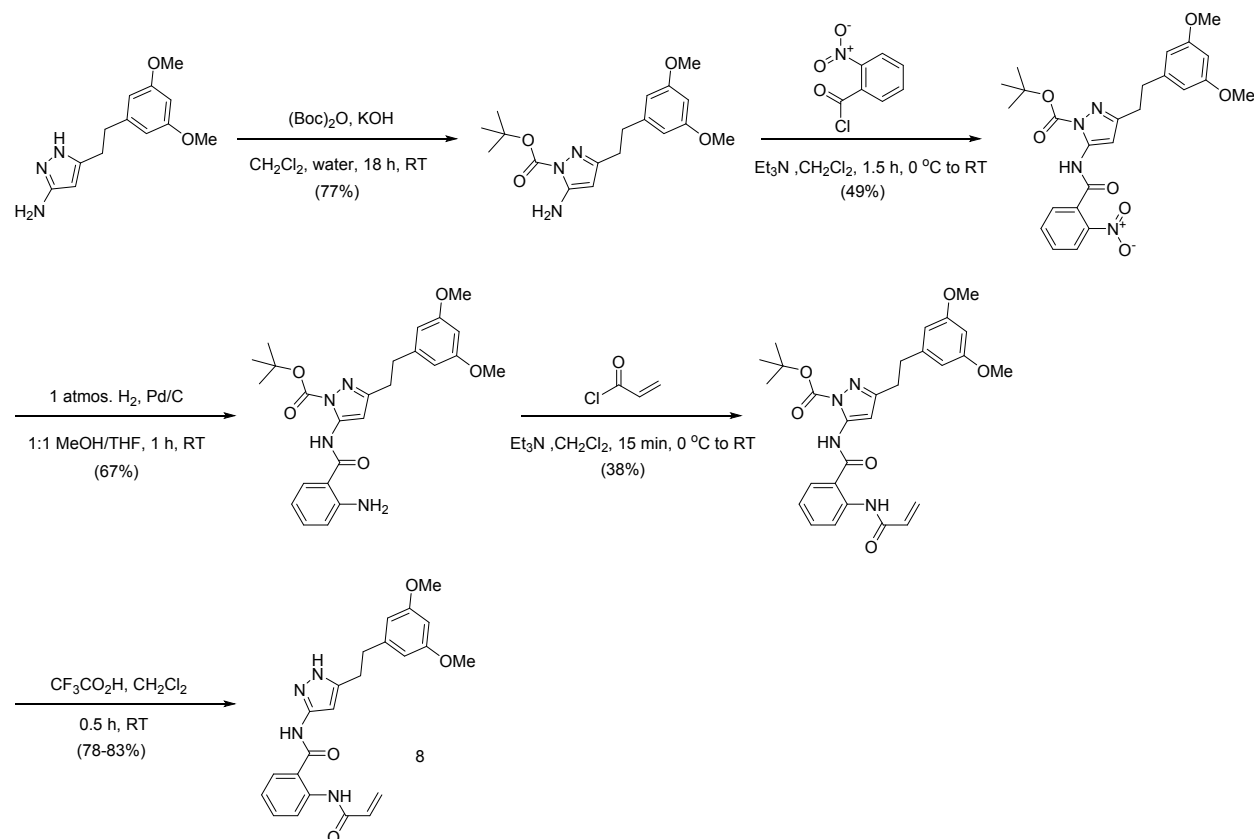
yield), which was used without further purification. ^1H NMR (400 MHz, $\text{DMSO-}d_6$) δ 0.97 (d, $J = 6.6$ Hz, 6 H), 2.03 (m, 1 H), 3.95 (d, $J = 6.4$ Hz, 2 H), 6.91 - 6.99 (m, 1 H), 7.26 - 7.34 (m, 1 H), 8.01 (dd, $J = 9.1, 6.1$ Hz, 1 H).

Step 3: 1-(3-isobutoxy-4-nitrophenyl)-*N,N*-dimethylpiperidin-4-amine. A solution of 4-fluoro-2-isobutoxy-1-nitrobenzene (1.5 g, 7.04 mmol) and 4-dimethylaminopiperidine (2.26 g, 17.59 mmol) in DMF (14 ml) was heated to 60 °C and stirred for 1 h. The reaction was cooled to RT, diluted with Et_2O , washed with saturates aqueous NaHCO_3 , water and brine, dried over Na_2SO_4 filtered and concentrated. The residue was dried under vacuum to give the desired product (2.19 g, 97 % yield) as an orange oil, which solidified upon standing to give a yellow solid. ^1H NMR (400 MHz, $\text{DMSO-}d_6$) δ 1.02 (d, $J = 6.6$ Hz, 6H), 1.39 (qd, $J = 11.8, 3.9$ Hz, 6H), 1.82 (d, $J = 12.5$ Hz, 2H), 1.97 - 2.12 (m, 2H), 2.18 (s, 6H), 2.28 - 2.40 (m, 1H), 2.95 (m, $J = 2.2$ Hz, 3H), 3.91 (d, $J = 6.4$ Hz, 2H), 4.02 (d, $J = 13.2$ Hz, 7H), 6.48 (d, $J = 2.5$ Hz, 3H), 6.57 (dd, $J = 9.5, 2.5$ Hz, 3H), 7.87 (d, $J = 9.3$ Hz, 3H).

Step 4: 1-(4-amino-3-isobutoxyphenyl)-*N,N*-dimethylpiperidin-4-amine. A solution of 1-(3-isobutoxy-4-nitrophenyl)-*N,N*-dimethylpiperidin-4-amine (2.19 g, 6.81 mmol) in MeOH (25 ml) and THF (25 ml) under argon was treated with Pd/C (0.218 g, 0.204 mmol), the flask was flushed with H_2 and the reaction mixture was stirred under a positive pressure of H_2 (balloon) for 2 h. The flask was flushed with argon for 5 minutes. The suspension was then filtered and concentrated under vacuum to give the desired product (1.93 g, 92 % yield) as a brown-purple solid. ^1H NMR (400 MHz, $\text{DMSO-}d_6$) δ 1.00 (d, $J = 6.85$ Hz, 6H), 1.48 (qd, $J = 11.8, 3.9$ Hz, 2H), 1.74 - 1.86 (m, 2H), 1.95 - 2.14 (m, 2H), 2.19 (s, 6H), 3.40 (d, $J = 12.2$ Hz, 2 H), 3.69 (d, $J = 6.4$ Hz, 2H), 4.16 (s, 2H), 6.29 (dd, $J = 8.3, 2.5$ Hz, 1H), 6.46 (d, $J = 2.5$ Hz, 1H), 6.52 (d, $J = 8.6$ Hz, 1H).

Step 5: (1*S*,2*S*,3*R*,4*R*)-3-(5-cyano-4-(4-(4-(dimethylamino)piperidin-1-yl)-2-isobutoxyphenylamino)-pyrimidin-2-ylamino)bicyclo[2.2.1]hept-5-ene-2-carboxamide 7. A mixture of (1*S*,2*S*,3*R*,4*R*)-3-(2-chloro-5-cyanopyrimidin-4-ylamino)bicyclo[2.2.1]hept-5-ene-2-carboxamide (47 mg, 0.163 mmol) and 1-(4-amino-3-isobutoxyphenyl)-*N,N*-dimethylpiperidin-4-amine (50 mg, 163 mmol) in ethylene glycol monomethyl ether (0.33 ml) was heated to 80 °C for 4.5 h. Saturated aq NaHCO_3 solution was added to the cooled reaction mixture, which was then extracted 3x with CH_2Cl_2 , the combined organic extracts dried over Na_2SO_4 and evaporated. The crude product was purified by normal phase chromatography, eluting with a gradient from CH_2Cl_2 to 10% methanol in CH_2Cl_2 containing 0.5% Et_3N , to give the desired product (78 mg, 79%). ^1H NMR (400 MHz, $\text{DMSO-}d_6$) δ 8.24 (s, 2H), 7.78 (s, 1H), 7.62 (s, 1H), 7.30 (br, s, 1H), 6.58 (br, s, 1H), 6.46 (dd, $J = 8.6, 2.5$ Hz, 1H), 6.28 (br, s, 1H), 6.11 (br, s, 1H), 3.82 (br, s, 1H), 3.75 - 3.67 (m, 4H), 2.84 (s, 1H), 2.73 (s, 1H), 2.69 - 2.56 (m, 2H), 2.42 (m, 1H), 2.20 (s, 7H), 1.97 (br, m, 2H), 1.82 (br, m, 2H), 1.47 (tt, $J = 12.3, 6.2$ Hz, 2H), 1.34 (d, $J = 8.7$ Hz, 1H), 1.22 (s, 1H), 0.91 (d, $J = 6.6$ Hz, 6H).

Compound 8 was prepared as outlined below.



Step 1: *tert*-butyl 5-amino-3-(3,5-dimethoxyphenethyl)-1*H*-pyrazole-1-carboxylate. Di-*tert*-butyl dicarbonate (3.2 ml, 13.8 mmol) was added to a biphasic mixture of 5-(3,5-dimethoxyphenethyl)-1*H*-pyrazol-3-amine (3.0 g, 12.1 mmol), in CH₂Cl₂ (120 ml) and aqueous KOH (25 ml 4M, 100 mmol) at room temperature and stirred for 18 hours. The phases were separated and the organic layer washed with water then brine, dried over Na₂SO₄ and evaporated. The crude product was purified by normal phase chromatography, eluting with a gradient from heptane to 1:1 EtOAc/heptane, to give the desired product as an off-white solid (3.43 g, 77% yield). ¹H NMR (500 MHz, CDCl₃) δ 1.68 (s, 9H), 2.88 (br, s, 4H), 3.80 (s, 6H), 5.29 (s, 2H), 6.34 (s, 1H), 6.42 (d, *J* = 1.6 Hz, 2H).

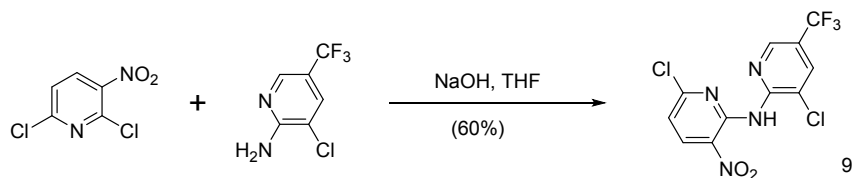
Step 2: *tert*-butyl 3-(3,5-dimethoxyphenethyl)-5-(2-nitrobenzamido)-1*H*-pyrazole-1-carboxylate. 2-Nitrobenzoylchloride (1.27 ml, 9.39 mmol) was added dropwise to a solution of *tert*-butyl 5-amino-3-(3,5-dimethoxyphenethyl)-1*H*-pyrazole-1-carboxylate (3.42 g, 9.34 mmol) and Et₃N (2.0 ml, 14.4 mmol) in CH₂Cl₂, (72 ml) cooled with an ice bath. The ice bath was removed and the mixture stirred for 1.5 hours at RT, then partitioned between saturated NaHCO₃ and CH₂Cl₂, extracted 1x with CH₂Cl₂, the combined organic layers dried over Na₂SO₄ and evaporated. The crude product was purified by normal phase chromatography, eluting with a gradient from heptane to 3:1 EtOAc/heptane, to give the desired product as an off-white solid (2.39 g, 49% yield). ¹H NMR (400 MHz, CDCl₃) δ 1.64 (s, 9H), 2.95 (s, 4H), 3.77 - 3.79 (m, 6 H), 6.32 (t, *J* = 2.4 Hz, 1H), 6.42 (d, *J* = 2.4 Hz, 2H), 6.92 (s, 1H), 7.63 - 7.70 (m, 2H), 7.73 - 7.78 (m, 1H), 8.07 - 8.14 (m, 1H), 10.58 (br, s, 1H).

Step 3: *tert*-butyl 5-(2-aminobenzamido)-3-(3,5-dimethoxyphenethyl)-1*H*-pyrazole-1-carboxylate. A solution of *tert*-butyl 3-(3,5-dimethoxyphenethyl)-5-(2-nitrobenzamido)-1*H*-pyrazole-1-carboxylate (2.39 g, 4.81 mmol) in MeOH (25 ml) and THF (25 ml) under argon was treated with Pd/C (0.25 g), the flask was flushed with H₂ and the reaction mixture was shaken under a positive pressure of H₂ (0.1 bar) for 1 h. The flask was flushed with argon for 5 minutes, and the suspension was then filtered and concentrated under vacuum. The crude product was purified by normal phase chromatography, eluting with a gradient from heptane to 7:8 EtOAc/heptane, to give the desired product as a white solid (1.54 g, 67 % yield). ¹H NMR (400 MHz, CDCl₃) δ 1.70 (s, 9H), 2.95 (s, 4H), 3.76 - 3.80 (m, 6H), 6.30 - 6.34 (m, 1H), 6.42 (d, *J* = 2.4 Hz, 2H), 6.80 - 6.88 (m, 3H), 7.29 - 7.35 (m, 1H), 7.54 (d, *J* = 7.8 Hz, 1H), 11.02 - 11.11 (m, 1H).

Step 4: *tert*-butyl 3-(2-acrylamidobenzamido)-5-(3,5-dimethoxyphenethyl)-1*H*-pyrazole-1-carboxylate. 2-Acryloylchloride (0.40 ml, 4.95 mmol) was added dropwise to a solution of *tert*-butyl 5-(2-aminobenzamido)-3-(3,5-dimethoxyphenethyl)-1*H*-pyrazole-1-carboxylate (1.54 g, 3.31 mmol) and Et₃N (1.0 ml, 7.21 mmol) in CH₂Cl₂, (10 ml) at room temperature. The reaction mixture was stirred for 15 minutes, then partitioned between saturated NaHCO₃ and CH₂Cl₂, extracted 3x with CH₂Cl₂, the combined organic layers dried over Na₂SO₄ and evaporated. The crude product was purified by normal phase chromatography, eluting with a gradient from heptane to 7:3 EtOAc/heptane, to give the desired product as an off-white solid (0.67 g, 38% yield). ¹H NMR (400 MHz, CDCl₃) δ 11.36 - 11.47 (m, 1H), 11.26 (s, 1H), 8.82 (d, *J* = 8.2 Hz, 1H), 7.69 (dd, *J* = 7.8, 1.2 Hz, 1H), 7.55 - 7.61 (m, 1H), 7.22 (s, 1H), 6.88 (s, 1H), 6.41 - 6.45 (m, 3H), 6.29 - 6.38 (m, 2H), 5.80 (dd, *J* = 10.0, 1.4 Hz, 1H), 3.78 (s, 6H), 2.97 (s, 4H), 1.70 (s, 9H).

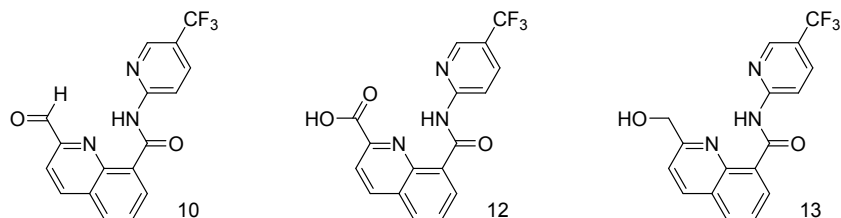
Step 5: 2-acrylamido-*N*-(5-(3,5-dimethoxyphenethyl)-1*H*-pyrazol-3-yl)benzamide **8**. Trifluoroacetic acid (1.5 ml, 19.5 mmol) was added to a solution of *tert*-butyl 3-(2-acrylamidobenzamido)-5-(3,5-dimethoxyphenethyl)-1*H*-pyrazole-1-carboxylate (673 mg, 1.29 mmol) in CH₂Cl₂, cooled with an ice bath. The reaction mixture was stirred for 30 minutes, then partitioned between saturated NaHCO₃ and CH₂Cl₂, extracted 3x with CH₂Cl₂, the combined organic layers were washed with water, dried over Na₂SO₄ and evaporated. The crude product was suspended in *i*Pr₂O (50 ml) and heated with sonication, then cooled and filtered to give the desired product as a white crystalline solid (430 mg, 78 % yield). ¹H NMR (400 MHz, DMSO-*d*₆) δ 12.21 (s, 1H), 11.06 (s, 1H), 10.86 (s, 1H), 8.32 (d, *J* = 8.3 Hz, 1H), 7.84 (d, *J* = 7.7 Hz, 1H), 7.57 - 7.45 (m, 1H), 7.17 (t, *J* = 7.6 Hz, 1H), 6.52 - 6.27 (m, 5H), 6.21 (dd, *J* = 16.9, 1.8 Hz, 1H), 5.78 (dd, *J* = 10.0, 1.7 Hz, 1H), 3.69 (s, 6H).

Compound 9 was prepared as outlined below.



3-chloro-N-(6-chloro-3-nitropyridin-2-yl)-5-(trifluoromethyl)pyridin-2-amine 9. A solution of 2,6-dichloro-3-nitropyridine (1.9 g, 10 mmol) was added dropwise over 30 minutes to a suspension of powdered potassium hydroxide (1.2 g, 20 mmol) in a solution of 3-chloro-5-(trifluoromethyl)pyridin-2-amine (1.9 g, 10 mmol) in THF (40 ml) at 0 °C. The reaction mixture was allowed to warm to room temperature, diluted with water (100 ml), and the pH adjusted to 2-3 by the addition of conc. hydrochloric acid. The mixture was extracted 4x with EtOAc, the combined organic layers washed with water, dried over MgSO₄, and evaporated. Purification of the crude product was carried out by normal phase chromatography (250 g Kieselgel), eluting with 1:3 diethyl ether/hexane, to give the desired product as a yellow crystalline solid (2.1 g, 60% yield). M.P. 70-71 °C. ¹H NMR (400 MHz, CDCl₃) δ 10.35 (br, s, 1H), 8.58 - 8.69 (m, 1H), 8.49 (dd, *J* = 8.6, 1.2 Hz, 1H), 8.00 (d, *J* = 2.4 Hz, 1H), 7.08 (dd, *J* = 8.6, 1.2 Hz, 1H).

Compounds **10**, **12** and **13** were prepared as described previously.^{S2} The acid **12** is obtained as an over oxidation product in the selenium dioxide oxidation used to prepare **10**.

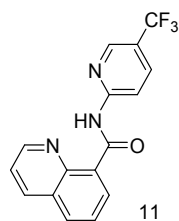


2-Formyl-N-(5-(trifluoromethyl)pyridin-2-yl)quinoline-8-carboxamide 10: white solid; ¹H NMR (400 MHz, DMSO-*d*₆) δ 13.79 (s, 1H), 10.18 (s, 1H), 8.94 – 8.68 (m, 3H), 8.52 (d, *J* = 8.8 Hz, 1H), 8.45 – 8.34 (m, 1H), 8.28 (dd, *J* = 8.9, 2.4 Hz, 1H), 8.14 (d, *J* = 8.5 Hz, 1H), 7.96 (t, *J* = 7.8 Hz, 1H).

8-((5-(Trifluoromethyl)pyridin-2-yl)carbamoyl)quinoline-2-carboxylic acid 12: white solid; ¹H NMR (400 MHz, DMSO-*d*₆) δ 13.76 (s, 1H), 9.01 – 8.66 (m, 3H), 8.56 (d, *J* = 8.8 Hz, 1H), 8.41 (d, *J* = 8.1 Hz, 1H), 8.28 (d, *J* = 8.7 Hz, 2H), 7.95 (t, *J* = 7.8 Hz, 1H).

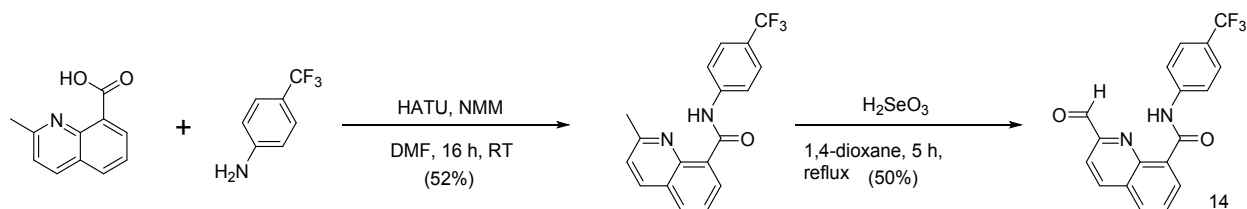
2-(Hydroxymethyl)-N-(5-(trifluoromethyl)pyridin-2-yl)quinoline-8-carboxamide 13: white solid; ¹H NMR (400 MHz, DMSO-*d*₆) δ 14.54 (s, 1H), 8.89 – 8.70 (m, 2H), 8.64 (d, *J* = 8.5 Hz, 1H), 8.54 (d, *J* = 8.8 Hz, 1H), 8.28 (ddd, *J* = 19.1, 8.5, 2.1 Hz, 2H), 7.92 – 7.74 (m, 2H), 5.82 (t, *J* = 5.9 Hz, 1H), 4.92 (d, *J* = 6.0 Hz, 2H).

Compounds **11** was prepared as described previously.^{S3}



N-(5-(Trifluoromethyl)pyridin-2-yl)quinoline-8-carboxamide 11: white solid; ¹H NMR (400 MHz, DMSO-*d*₆) δ 14.27 (s, 1H), 9.16 (dd, *J* = 4.3, 1.8 Hz, 1H), 8.85 – 8.72 (m, 2H), 8.66 (dd, *J* = 8.4, 1.8 Hz, 1H), 8.56 (d, *J* = 8.7 Hz, 1H), 8.30 (ddd, *J* = 28.0, 8.5, 2.1 Hz, 2H), 7.90 – 7.68 (m, 2H).

Compounds 14 was prepared as outlined below:

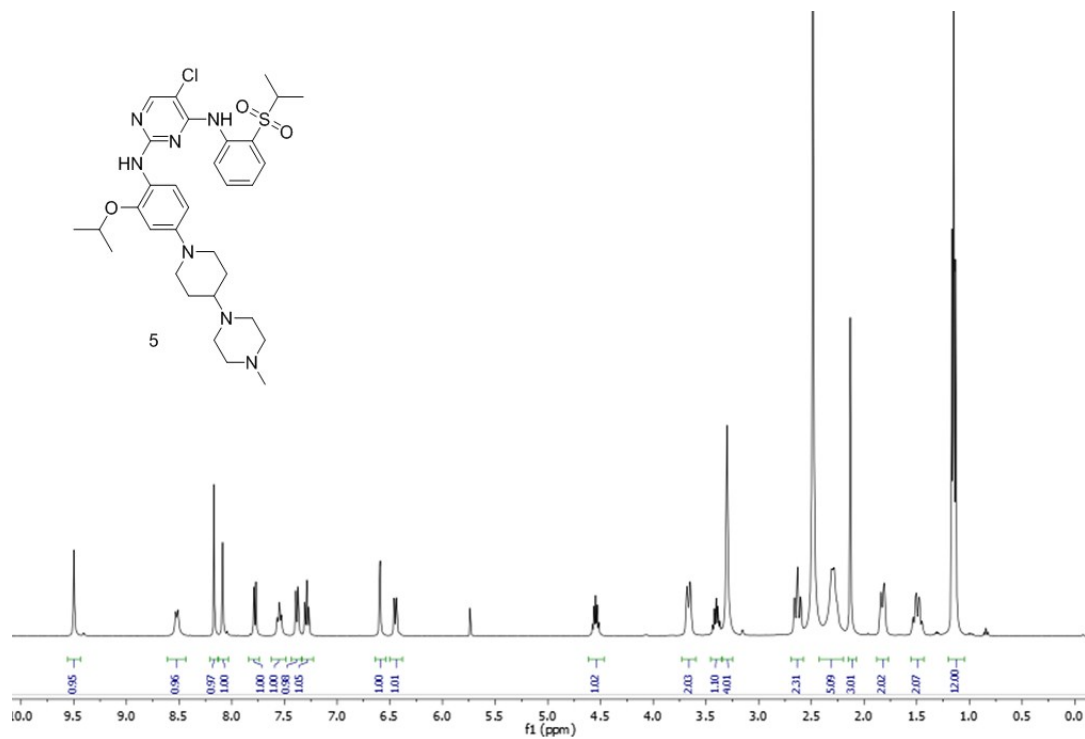


Step 1: 2-methyl-N-(4-(trifluoromethyl)phenyl)quinoline-8-carboxamide. A mixture of 2-methylquinoline-8-carboxylic acid (50 mg, 0.267 mmol), 4-(trifluoromethyl)aniline (43 mg, 0.267 mmol), HATU (102 mg, 0.267 mmol), and *N*-methyl morpholine (29 μ l, 0.267 mmol) in DMF (2 ml) was stirred at RT for 16 hours. The reaction mixture was diluted with EtOAc, washed 2x with saturated aqueous NaHCO₃ and 1x with brine, the organic phase dried over Na₂SO₄ and evaporated. The crude product was purified by normal phase chromatography, eluting with a gradient from heptane to 1:3 EtOAc/heptane, to give the desired product as a white solid (48 mg, 52% yield). ¹H NMR (400 MHz, DMSO-*d*₆) δ 2.90 (s, 3H), 7.59 - 7.70 (m, 1H), 7.73 - 7.85 (m, 1H), 8.07 (s, 1H), 8.20 - 8.33 (m, 1H), 8.48 - 8.60 (m, 1H), 8.63 - 8.73 (m, 1H), 13.83 - 14.26 (m, 1H), 13.94 - 14.17 (m, 1H).

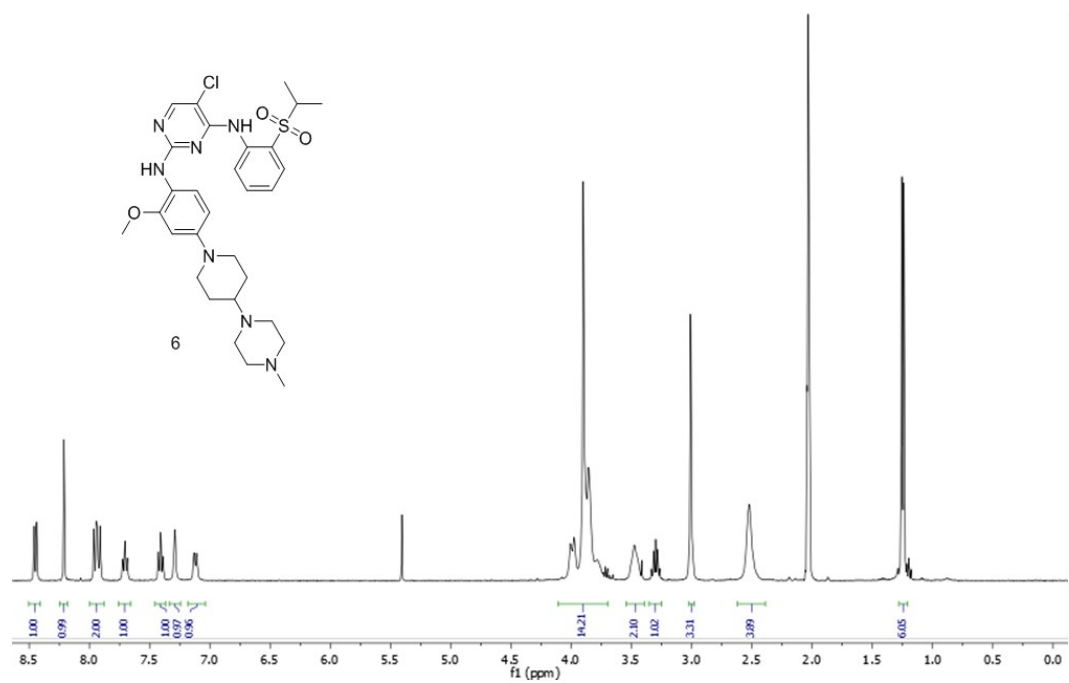
Step 2: 2-formyl-N-(4-(trifluoromethyl)phenyl)quinoline-8-carboxamide 14. Selenous acid (37 mg, 0.289 mmol) was added to a solution of 2-methyl-N-(4-(trifluoromethyl)phenyl)quinoline-8-carboxamide (48 mg, 0.145 mmol) in 1,4-dioxane (4 ml), and the mixture heated at reflux under N₂ for 5 hours. The reaction mixture was diluted with EtOAc, washed 2x with saturated aqueous NaHCO₃ and 1x with brine, the organic phase dried over Na₂SO₄ and evaporated. The crude product was purified by normal phase chromatography, eluting with a gradient from heptane to 7:3 EtOAc/heptane, to give the desired product as a beige solid (26 mg, 50% yield). ¹H NMR (400 MHz, DMSO-*d*₆) δ 12.93 (s, 1H), 10.29 (s, 1H), 8.87 (d, *J* = 8.4 Hz, 1H), 8.74 - 8.64 (m, 1H), 8.46 - 8.37 (m, 1H), 8.19 (dd, *J* = 14.9, 8.4 Hz, 3H), 7.99 (t, *J* = 7.7 Hz, 1H), 7.80 (d, *J* = 8.4 Hz, 2H).

2 NMR spectra

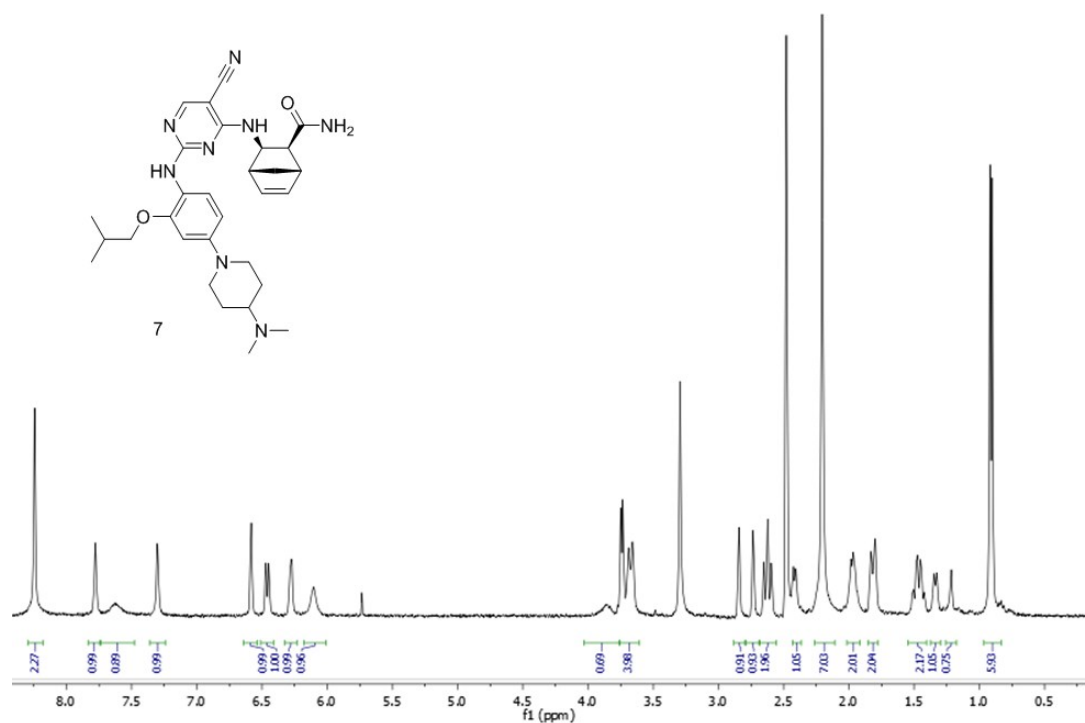
400 MHz ^1H NMR of 5 in $\text{DMSO-}d_6$



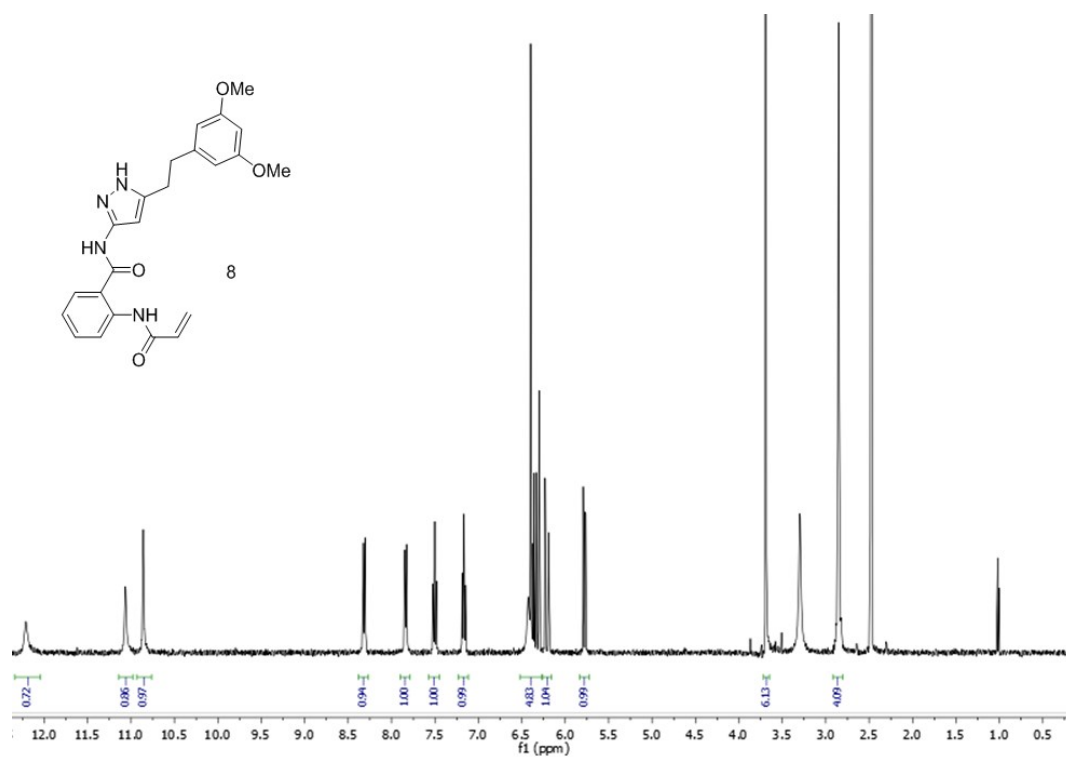
400 MHz ^1H NMR of 6 in acetic acid- d_4



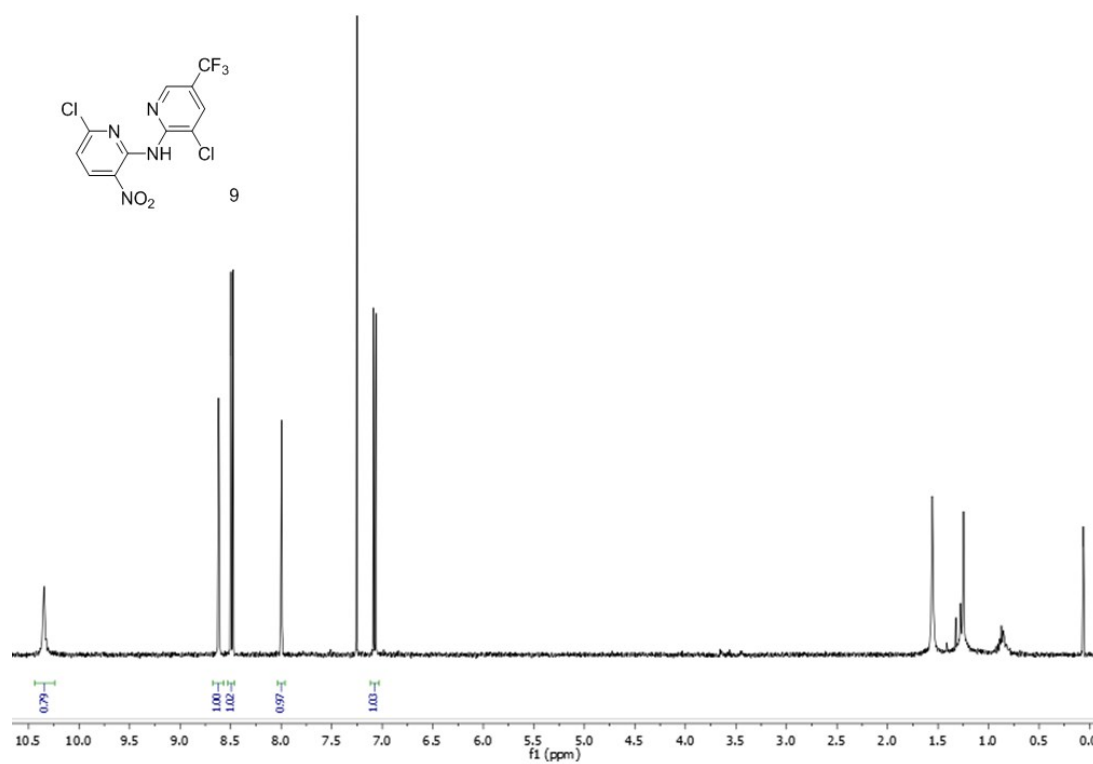
400 MHz ^1H NMR of 7 in $\text{DMSO-}d_6$



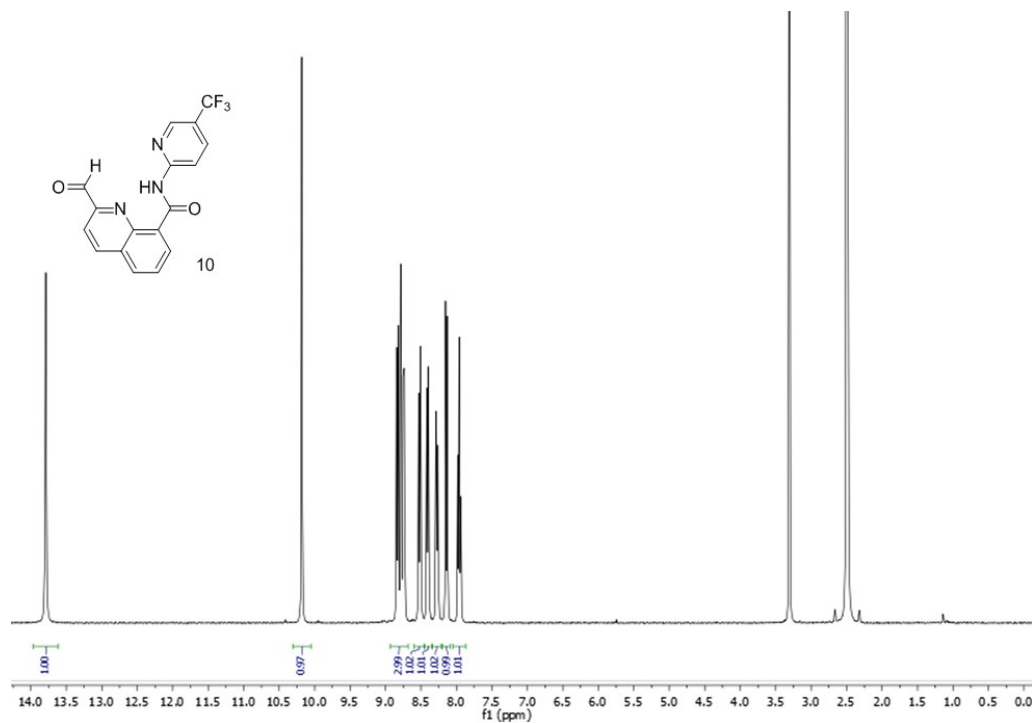
400 MHz ^1H NMR of 8 in $\text{DMSO-}d_6$



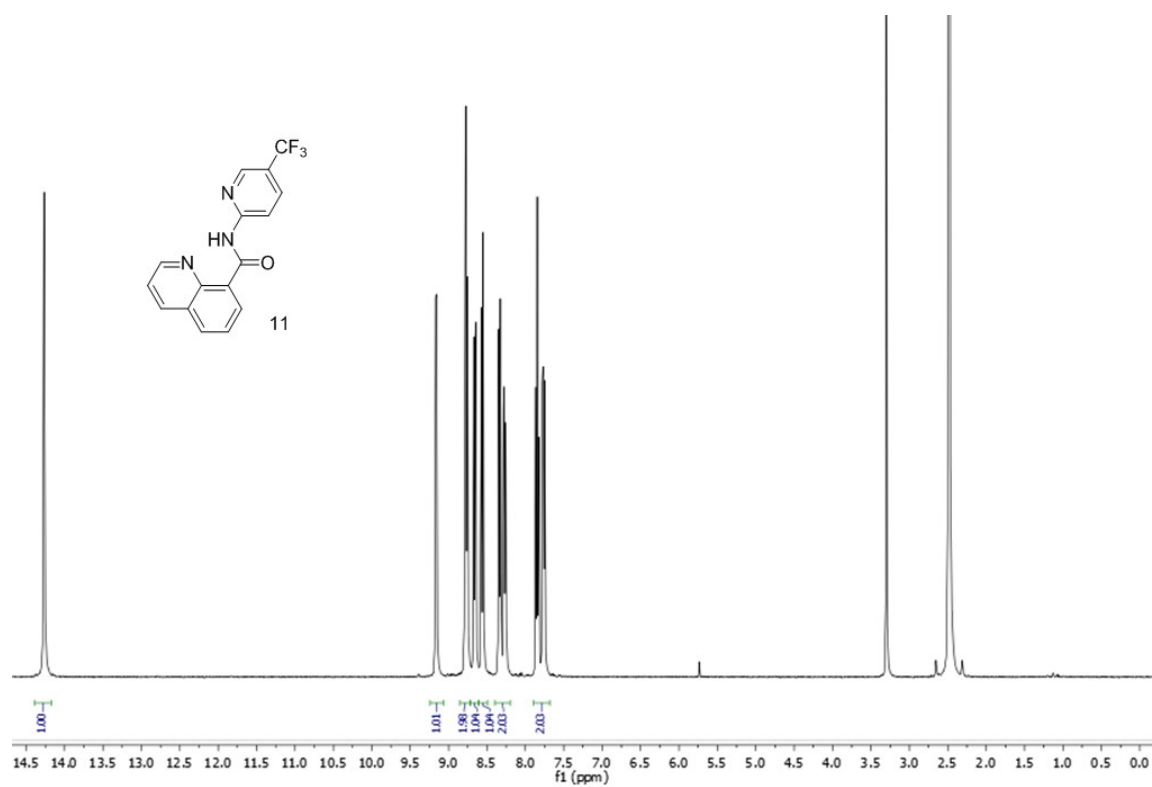
400 MHz ^1H NMR of 9 in CDCl_3



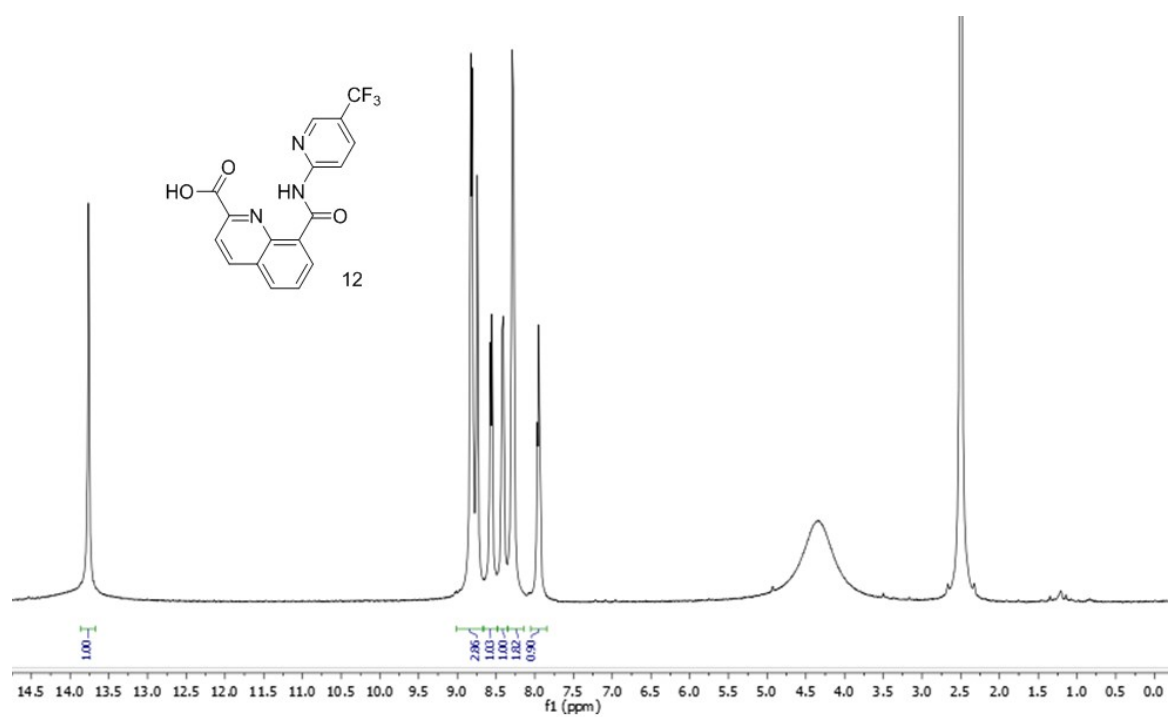
400 MHz ^1H NMR of 10 in $\text{DMSO}-d_6$



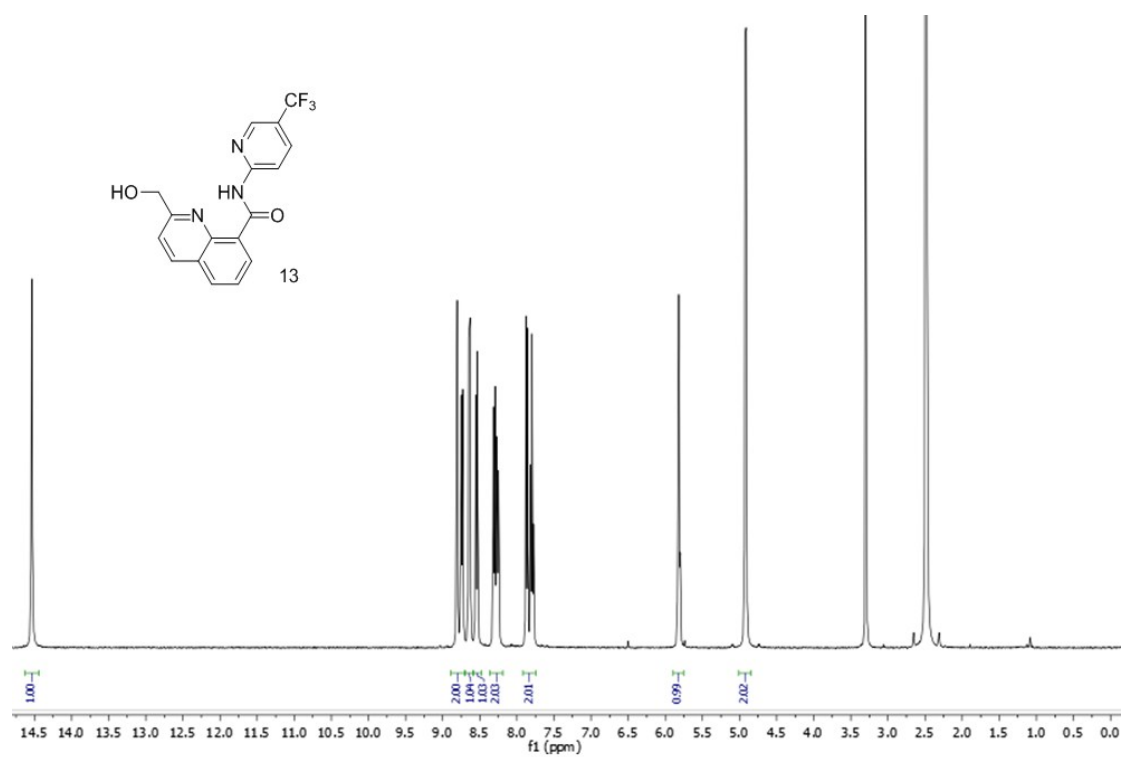
400 MHz ^1H NMR of 11 in $\text{DMSO-}d_6$



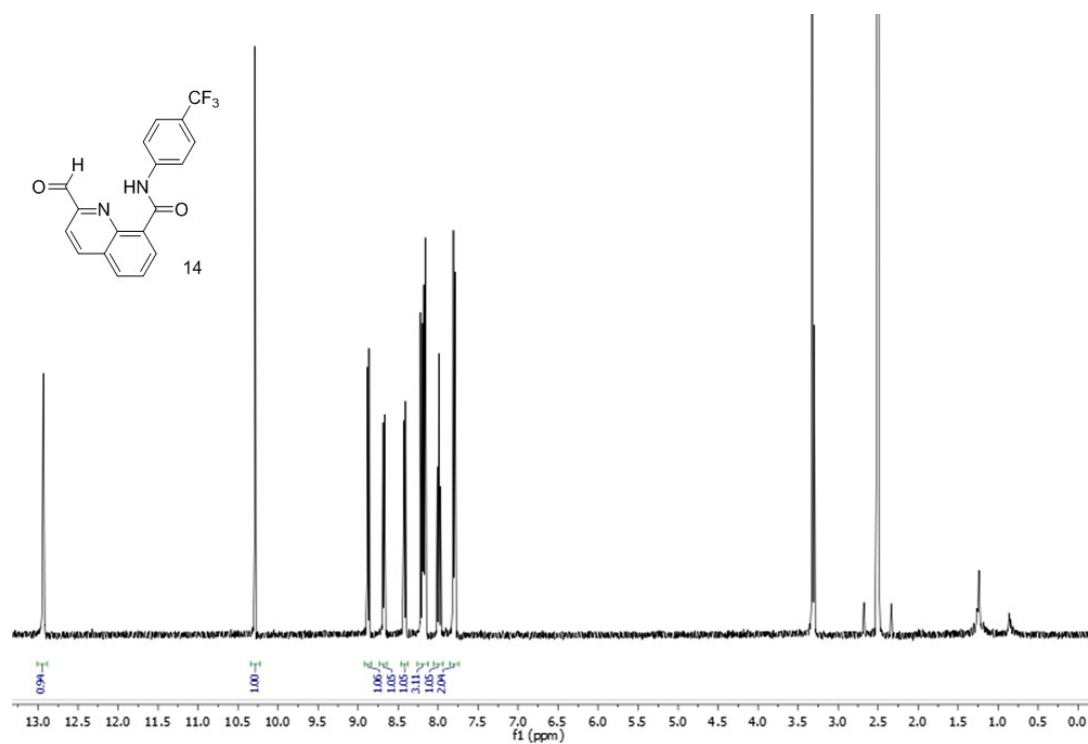
400 MHz ^1H NMR of 12 in $\text{DMSO-}d_6$



400 MHz ^1H NMR of 13 in $\text{DMSO-}d_6$



400 MHz ^1H NMR of 14 in $\text{DMSO-}d_6$



3 Molecular modeling

At the initiation of this project, no crystal structure of the kinase domain of FGFR4 was available. Therefore, to support the project a model of this domain was generated by homology to the crystal structure of infigratinib in complex with FGFR1 (PDB code: 3TT0). The sequences of the human FGFR1 and FGFR4 kinases were obtained from SWISS-PROT,⁵⁴ entries P11362 and P22455, respectively. The sequences were aligned using T-Coffe.⁵⁵ On the basis of the resulting alignment, the 3D structure of the FGFR4 kinase was modeled using the 'WHAT IF' program with the default parameters (PIRPSQ module, BLDPIR command).⁵⁶ Modeling and docking using the homology model was performed with a version of MacroModel enhanced for graphics by A. Dietrich.⁵⁷ The compounds were manually constructed and docked in the ATP site of the model and the resulting ligand-protein complexes energy-minimized using the AMBER*/H₂O/GBSA force field.

Ab initio conformational calculations for compound **10** were performed in Jaguar (Schrödinger Inc.) at the B3LYP/6-31G** level with full geometry optimization. The figures for the structural models were prepared using PYMOL (Schrodinger, Inc.).

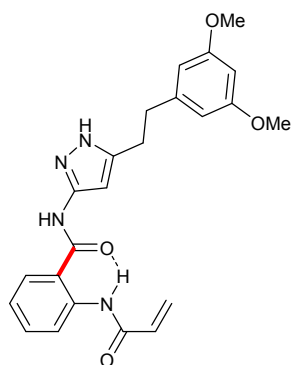


Figure S1. Lowest energy amide conformers of **8**.

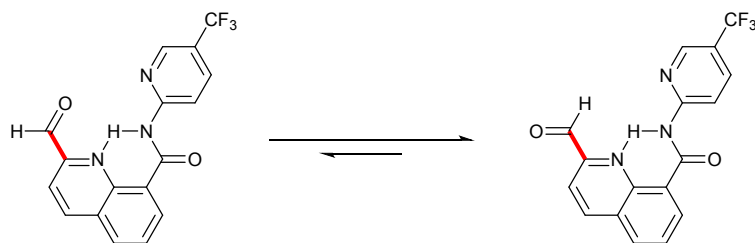


Figure S2. Aldehyde conformers of **10** assessed by Ab initio calculations.

Modeling the interactions of **6** and **7** with the C552A variant of FGFR4

The above structure of FGFR4 in which the cysteine at position 552 was switched for alanine was used to model the interactions with compounds **6** and **7**. In contrast to the methoxy analogue **6**, the isobutoxy analogue **7** is able to fill the additional space created by the C552A variant to maintain the hydrophobic surface shielding the hinge interaction.

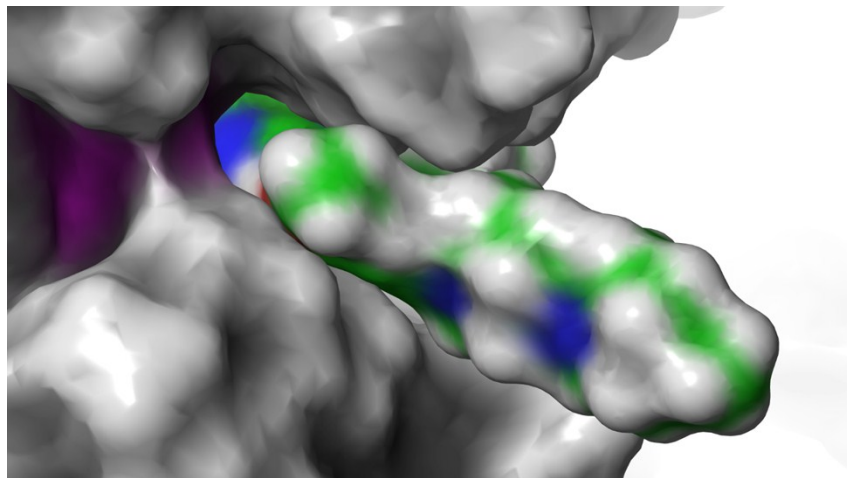


Figure S3. Model of **6** bound into the C552A variant of FGFR4. The carbon atoms of **6** are highlighted in green and Ala552 is highlighted purple.

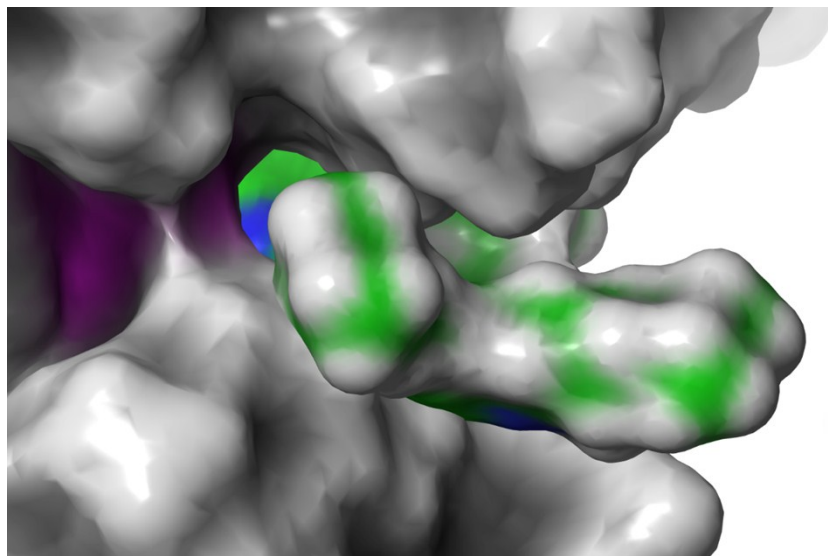


Figure S4. Model of **7** bound into the C552A variant of FGFR4. The carbon atoms of **7** are highlighted in green and Ala552 is highlighted purple.

Modeling the covalent binding of **8** to Cys552

The above structure of FGFR4 was used to model the covalent adduct with **8** following a Michael reaction with Cys552, and the minimised structure is shown in Figure S5 below. Following the thioether formation the key interactions with the hinge and back-pocket, made by the parent compound, are retained in the adduct, as outlined in Figure 8 in the main text for the Cys477 covalent adduct.

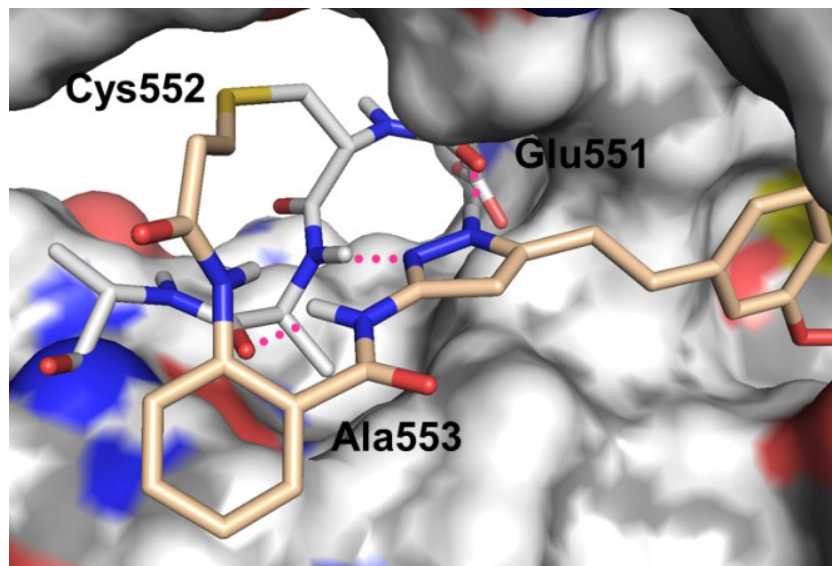


Figure S5. Model of **8** covalently bound to the middle-hinge Cys552 of the FGFR4 kinase domain.

Modeling the covalent binding of **9** to Cys477

The above structure of FGFR4 was used to model the covalent adduct with **9** following a S_NAr reaction with Cys477 in two conformations: 1) with the P-loop in the active hairpin conformation; 2) with the P-loop in the disordered conformation found in the X-ray structure of **8**, shown in Figure 8 in the main text. The minimised structures are shown in Figure S6, and in neither of the structures does the bipyridyl moiety interact within the ATP-pocket.

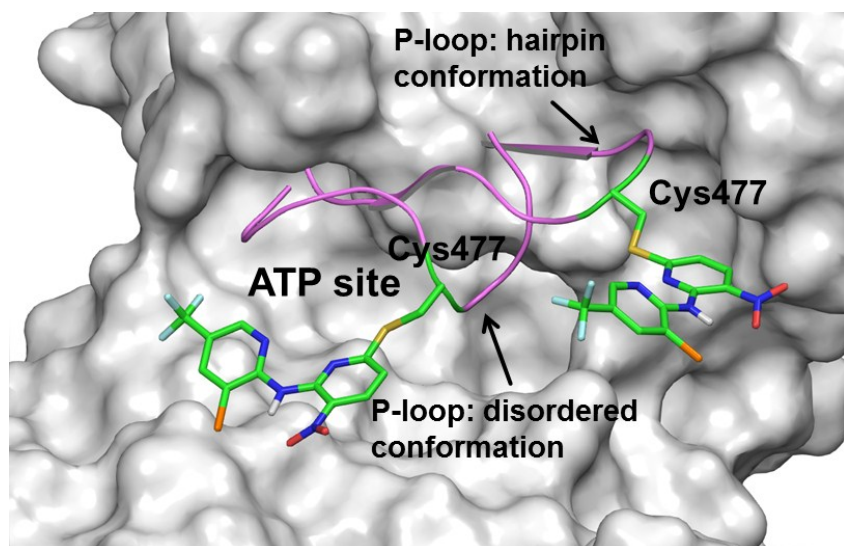


Figure S6: Models of compound **9** bound to FGFR4 after reaction with Cys477 considering two possible conformations of the P-loop.

4 Biochemical FGFR screening

The biochemical assays used to assess the FGFR family and FGFR4 cysteine to alanine variant activities are described below. MS studies with the FGFR1 (407-822), FGFR2 (406-821), FGFR3 (411-806) and FGFR4 (388-802) kinase domains revealed them to contain the proteins as mixtures of phosphorylation states (Table 1 in the main text). The FGFR4 (442-753), (442-C477A-753) and (442-C552A-753) constructs were fully dephosphorylated during the isolation and purification sequence (Table 2 in the main text).

Generation of the non-phosphorylated FGFR4 442-753 kinase domain proteins

Cloning: The boundary corresponding to kinase domain of FGFR4 (G442-E753), with or without point mutation, was codon optimized for expression in *Spodoptera frugiperda* (Sf9) insect cells. The gene was synthesized and cloned in flashBac compatible transfer vector with HRV3c protease or TEV protease cleavable 6xHis in *N*-terminus.

Transfection and Virus generation: Sf9 insect cells were co-transfected with construct DNA (gene of interest in transfer vector) and flashBac DNA using the protocol from supplier of flashBac (Oxford Expression Technologies). Virus generated were collected on day 5. Sf9 cells (3 ml) grown and maintained in log phase (1.5×10^6 cell per ml) were infected with V0 virus (120 μ l) and incubated at 27 °C for 48 h with 200 rpm in a shaker incubator. Culture was aseptically centrifuged at 1500 rpm for 10 min to recover supernatant as V1 virus stock. Working stock of virus was generated by infecting 100 ml of Sf9 cells in log phase with 100 μ l of V1 virus. Culture was centrifuged 48 h post infection and clear supernatant was stored at 4 °C as V2 virus stock.

Expression: 1 L of Sf9 cells at 2×10^6 cells per ml in a 3 L Erlenmeyer flask was infected with 10 ml of V2 virus generated above. Infected culture was incubated at 27 °C for 48 h with 90 rpm in a shaker incubator. Cell pellets were harvested by centrifuging the culture at 1500 rpm for 15 min and stored at -80 °C.

Purification: Pellet from 2 L of culture was thawed at room temperature and suspended in lysis buffer (50 mM Tris pH7.6, 400 mM NaCl, 10% Glycerol v/v, 3 mM TCEP supplemented with EDTA-free protease inhibitor, Roche). Each gram of pellet was suspended in 8 ml of lysis buffer. The suspension was homogenized by passing through a French press 3 times. Clarified supernatant was loaded on Ni-NTA Superflow Cartridge (Qiagen) using AKTA purifier system. Target protein was eluted using lysis buffer supplemented with 200 mM imidazole. His tag was removed by using appropriate protease cleavage and protein is dephosphorylated using Lambda phosphatase in presence of 2 mM $MnCl_2$. Partially purified protein is diluted to achieve final NaCl concentration to 100 mM in IEX buffer (20 mM Tris pH 7.6, 10% glycol, 1 mM TCEP) and loaded on MonoQ column and fractionated by using NaCl gradient from 100 to 400 mM in 20 column volume. Fraction corresponding to target protein was collected, concentrated and loaded on gel filtration column (HiLoad 16/60 Superdex 75 μ g) pre-equilibrated with 20 mM Tris pH7.6, 150 mM NaCl, 3 mM TCEP, 1 mM EDTA. Correct mass of the purified protein was determined by mass spectrometry. Aliquots are flash frozen and stored at -80 °C.

FGFR biochemical assays (Tables 1 and 2 in the main text): All assays were performed in 384-well small volume microtiter plates (Greiner bio-one, Cat. No. 784076). Each assay plate contained 8-point serial dilutions for 40 test compounds, as well as four 8-point serial dilutions of staurosporine as a reference compound, plus 16 high- and 16 low controls.

Liquid handling and incubation steps were done on an Innovadyne Nanodrop Express equipped with a robotic arm (Thermo CatX, Caliper Twister II) and an incubator (Liconic STX40, Thermo Cytomat 2C450). The assay plates were prepared by addition of 50 nl per well of compound solution in 90% DMSO. The kinase reactions were started by stepwise addition of 4.5 μ L per well of enzyme solution (50 mM HEPES pH 7.5, 1 mM DTT, 0.02% Tween20, 0.02% BSA, 10 mM beta-glycerolphosphate, 10 μ M sodium orthovanadate with enzyme specific enzyme / $MgCl_2$ / $MnCl_2$ concentrations, Table S1) and 4.5 μ L per well of peptide/ATP-solution (4 μ M peptide, FGFR1-3 assays used the 5-Fluo-Ahx-EEPLYWSFPAKKK-CONH₂ peptide substrate, and the FGFR4 assays used the 5-Fluo-Ahx-KKKKEEYFFFG-NH₂ peptide substrate, 50 mM HEPES pH 7.5, 1 mM DTT, 0.02% Tween20, 0.02% BSA, 10 mM beta-glycerolphosphate, 10 μ M sodium orthovanadate with enzyme specific ATP / $MgCl_2$ / $MnCl_2$ concentrations, Table S1). Kinase reactions were incubated at 30 °C for 60 minutes and subsequently terminated by addition of 15 μ L per well of stop solution (100 mM HEPES pH 7.5, 5% DMSO, 0.1% Caliper coating reagent, 10 mM EDTA, and 0.015% Brij35). Plates with terminated kinase reactions were transferred to the Caliper LC3000 system for reading. Phosphorylated and unphosphorylated peptides were separated using the Caliper microfluidic mobility shift technology. Briefly, samples from terminated kinase reactions were applied to the chip. Analytes are transported through the chip by constant buffer flow and the migration of the substrate peptide is monitored by the fluorescence signal of its label. Phosphorylated peptide (product) and unphosphorylated peptide (substrate) are separated in an electric field by their charge/mass ratio. Kinase activities were calculated from the amounts of formed phospho-peptide. IC₅₀ values were determined from percent inhibition values at different compound concentrations by non-linear regression analysis.

Table S1. Details of the biochemical assay conditions.

Kinase domain (sequence)	Enzyme conc (nM)	ATP K _m (μ M)	MgCl ₂ / MnCl ₂ conc (μ M)
FGFR1(407-822)	2	319	12 / 0
FGFR2 (406-821)	3	146	12 / 0
FGFR3(411-806)	0.25	353	12 / 0
FGFR4 (388-802)	3	561	16 / 0
FGFR4 (442-753) nonphos	3	220	18 / 2
FGFR4 (442-C477A-753) nonphos	3	161	20 / 2
FGFR4 (442-C552A-753) nonphos	5	789	16 / 3

High throughput screening campaign (HTS): A time-resolved fluorescence energy transfer (TR-FRET) assay was used in a 1536-well format with the non-phosphorylated wild-type FGFR4 kinase domain (442-753) to screen 1.4 million compounds at a concentration of 25 μ M. In more detail, the final assay volume was 5 μ L in buffer (50 mM Hepes, pH 7.4, 0.05% CHAPS, 0.02% bovine serum albumin, 1 mM dithiothreitol, 10 mM MgCl₂, 1 mM MnCl₂) which contained: 10 nM FGFR4; 50 μ M ATP; 500 nM biotin-

labelled CSKtide substrate; EDTA 10 mM; 5 nM streptavidin-allophycocyanin; 1.5 mM Eu-labelled anti-phosphotyrosine antibody. FGFR4 and test compounds were first incubated for 30 minutes before the addition of ATP, after a further 60 minutes the CSKtide substrate was added followed by the detection mix after a further 15 minute incubation. The plates were then read with a Perkin Elmer En Vision Multiplate Reader after a further 40 minute incubation period. From this screen 18.8 thousand hits were chosen for confirmation at four concentrations using the HTS FGFR4 assay and also the FGFR2 assay, described above, as a selectivity screen. Finally 4400 hits were selected for IC_{50} determinations using the FGFR4 and the FGFR2 assays.

Kinase selectivity profiles of compounds 5 – 10.

Biochemical kinase assays: Assays were performed with the indicated purified kinases, or recombinant kinase-domains, in the absence and with increasing concentrations of the test compounds by measuring the incorporation of ³³P, from [γ ³³P]ATP, into appropriate substrates. All values are from duplicate measurements, and average values are shown from 1 to 3 separate experiments, Table S2.

The Caliper assays are typically run at ATP K_m for the assay specific enzyme concentration.

Table S2. Biochemical kinase inhibitory activities for compounds 5 – 10.

Kinase	Compound IC ₅₀ values (μM)					
	5	6	7	8	9	10
ABL1	> 10	n.d.	> 10	> 10	> 10	> 10
ACVR1	> 10	n.d.	> 10	> 10	> 10	> 10
AKT1	n.d.	n.d.	> 10	> 10	> 10	4.1
AURKA	2.1	n.d.	1.9	2.3	> 10	> 10
BTK	> 10	n.d.	> 10	1.2	> 10	> 10
CAMK2D	n.d.	n.d.	0.019	> 10	n.d.	> 10
CDK1B	> 10	0.16	> 10	> 10	> 10	> 10
CDK2A	> 10	n.d.	> 10	> 10	> 10	> 10
CDK4D1	7.9	n.d.	5.9	> 10	> 10	> 10
CSK	> 10	n.d.	> 10	> 10	> 10	> 10
CSNK1G3	> 10	n.d.	3.9	> 10	> 10	> 10
EGFR	2.4	n.d.	0.051	> 10	> 10	> 10
EphA4	> 10	n.d.	n.d.	n.d.	n.d.	n.d.
EphB4	> 10	1.7	> 10	> 10	> 10	> 10
ERBB2	9.2	n.d.	0.25	n.d.	n.d.	n.d.
ERBB4	2.8	n.d.		3.9	> 10	> 10
FLT3-D835Y	3.6	0.13	0.37	> 10	> 10	> 10
FYN	> 10	n.d.	n.d.	n.d.	n.d.	n.d.
GSK3B	> 10	n.d.	> 10	> 10	> 10	> 10
HCK	> 10	n.d.	n.d.	n.d.	n.d.	n.d.
HER1	2.7	0.74	n.d.	n.d.	n.d.	n.d.
HER2	6.2	6.7	n.d.	n.d.	n.d.	n.d.
IGF1R	0.054	0.28	n.d.	n.d.	n.d.	n.d.
INSR	0.11	0.13	0.46	> 10	> 10	> 10
IRAK1	n.d.	n.d.	> 10	> 10	> 10	> 10
IRAK4	> 10	n.d.	> 10	> 10	> 10	> 10
JAK1	> 10	n.d.	> 10	> 10	> 10	> 10
JAK2	> 10	1.6	> 10	> 10	> 10	> 10
JAK3	> 10	5.8	n.d.	n.d.	n.d.	n.d.
KDR	> 10	0.093	0.54	4.3	> 10	> 10
KIT	> 10	n.d.	> 10	> 10	> 10	> 10
LCK	> 10	n.d.	> 10	> 10	> 10	> 10
LYN	> 10	n.d.	> 10	> 10	> 10	> 10
MAP3K8	> 10	n.d.	> 10	> 10	> 10	> 10
MAPK14	n.d.	n.d.	n.d.	n.d.	n.d.	n.d.
MAPK1	4.9	n.d.	8.3	> 10	> 10	> 10

MAPKAPK2	8.8	n.d.	> 10	> 10	2.1	2.3
MAPKAPK5	> 10	n.d.	1.4	n.d.	> 10	> 10
MERTK	3.1	n.d.	n.d.	n.d.	n.d.	> 10
MET	> 10	n.d.	> 10	> 10	> 10	> 10
MKNK1	> 10	n.d.	> 10	> 10	> 10	> 10
MKNK2	2.1	n.d.	1.5	> 10	> 10	> 10
PAK2	n.d.	n.d.	> 10	> 10	> 10	> 10
PDGFR α	> 10	0.91	n.d.	n.d.	n.d.	> 10
PDGFR α -V561D	> 10	n.d.	0.90	> 10	> 10	5.9
PDPK1	> 10	3.7	> 10	> 10	> 10	> 10
PIM2	> 10	n.d.	> 10	> 10	> 10	> 10
PKN1	> 10	n.d.	> 10	> 10	> 10	> 10
PKN2	> 10	n.d.	> 10	> 10	> 10	> 10
PLK1	3.4	n.d.	0.15	> 10	> 10	> 10
PRKACA	> 10	n.d.	> 10	> 10	> 10	> 10
PRKCA	> 10	n.d.	> 10	> 10	> 10	> 10
PRKCQ	> 10	n.d.	> 10	> 10	> 10	> 10
RET	> 10	1.7	8.8	> 10	> 10	> 10
ROCK2	7.3	n.d.	1.0	> 10	> 10	> 10
RPS6KB1	> 10	n.d.	> 10	> 10	> 10	> 10
SRC	> 10	n.d.	> 10	> 10	> 10	> 10
SYK	> 10	n.d.	> 10	> 10	n.d.	> 10
TYK2	> 10	n.d.	n.d.	n.d.	n.d.	n.d.
WNK1	> 10	n.d.	> 10	> 10	> 10	> 10
YES	5.2	n.d.	n.d.	n.d.	n.d.	n.d.
ZAP70	> 10	1.2	> 10	> 10	> 10	> 10

n.d. = not determined.

5 Selected profiling data for compound 7

The profile of compound **7** made it suitable for use as a selective non-covalent FGFR4 tool compound, and selected data are included below.

Compound **7** was a potent inhibitor of FGFR4-phosphorylation in an FGFR4-dependent Ba/F₃ cell line,⁵⁸ and inhibited proliferation of the FGF19/FGFR4 expressing HCC cell lines: HUH7, JHH7, and Hep3B. Data are shown in Table S3.

Table S3. Cellular FGFR4 inhibitory activities of compound **7**.

Assay	IC ₅₀ (nM)
FGFR4 Ba/F ₃ phosphorylation	162 ± 52
HUH7	237 ± 95
JHH7	282 ± 130
Hep3B	261 ± 230

Data are mean ± SD.

A pharmacokinetic study in the mouse was conducted as outlined below, and showed **7** to be orally bioavailable. Data are shown in Table S4 and Figures S7 and S8.

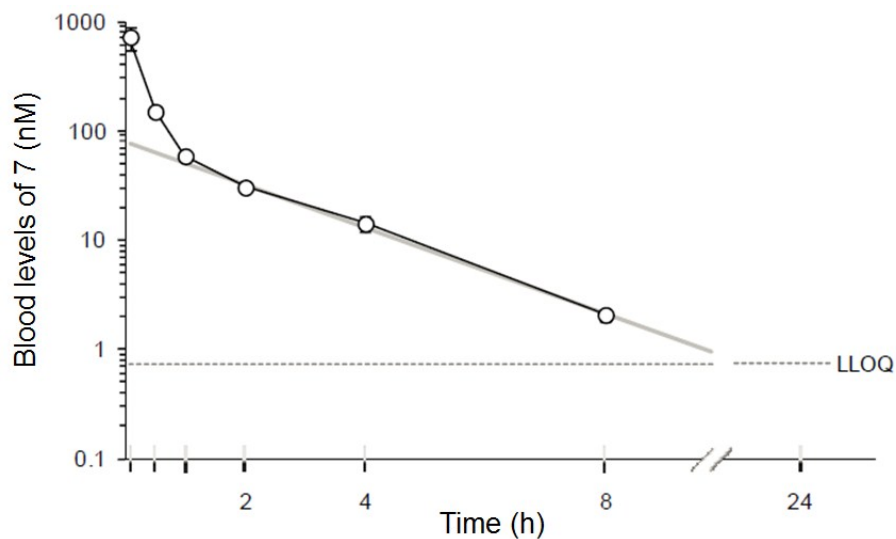
Method: The experiments were performed according to the regulations effective in the Canton Basel-Stadt, Switzerland, all procedures and protocols were reviewed and approved by the local veterinary authorities of the Canton Basel-Stadt, specifically according to experimental license No. BS1587. Species/Strain: Female mice (Balb/c). Sample collection: Blood (EDTA, once by sublingual bleeding approximately 70 µL/mouse and once at sacrifice approximately 300 µL/mouse) n=3 with 3 mice/sampling time. Sampling time points: i.v.: 0.08; 0.5; 1.0; 2.0; 4.0; 8.0; 24.0 h, and p.o.: 0.25; 0.5; 1.0; 2.0; 4.0; 8.0; 24.0 h. Matrix/Volume: approximately 50 µL blood. Application format: Discrete [single, one-in-one]. Dose i.v.: 1.0 mgkg⁻¹. Dose p.o.: 3.0 mgkg⁻¹. Formulation i.v.: Solution in NMP:Plasma (10:90), administration volume 5 mLkg⁻¹. Formulation p.o.: Suspension in Tween 80 : carboxymethyl cellulose 05 (0.5:99.5), administration volume 10 mLkg⁻¹. Extraction and sample preparation involved protein precipitation: 30 µL blood were mixed with 200 µL acetonitrile and centrifuged at 4 °C. Approximately 200 µL of supernatant were transferred into a microtiter plate and mixed with 200 µL of 0.1% formic acid. An aliquot of each sample was injected into the LC-MS/MS system for analysis. Data analysis was done using a non-compartmental approach.

Table S4: Blood pharmacokinetic parameters of **7** in conscious mice after i.v. and p.o. administration.

Clearance (mL·min ⁻¹ ·kg ⁻¹)	73
Volume of distribution at steady state (L·kg ⁻¹)	4.5
Terminal elimination half-life (h)	1.5
Mean residence time (h)	1.0
AUC i.v. d.n. (nM·h)	420
AUC p.o. d.n. (nM·h)	92
Oral bioavailability (%)	22
Maximum p.o. blood concentration d.n. (nM)	30
Time of peak blood concentration (h)	2.0

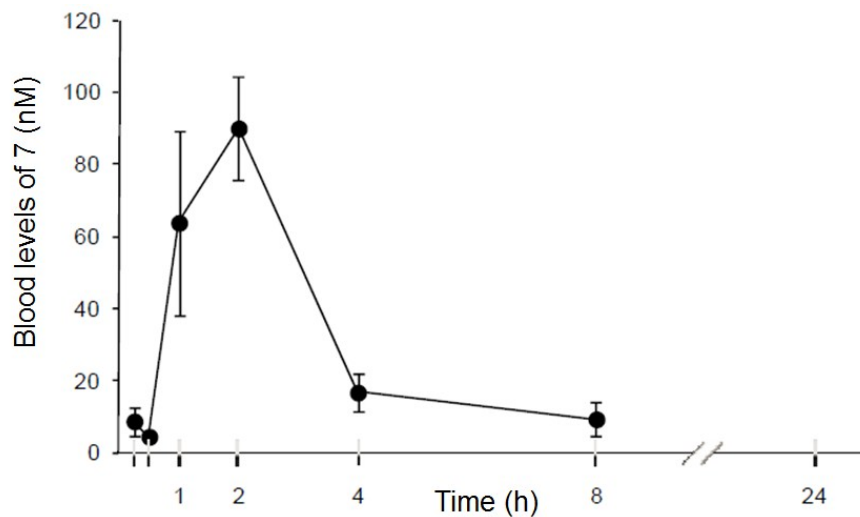
d.n. = dose-normalised to a dose of 1 mg·kg⁻¹

Figure S7: Pharmacokinetic profile of **7** in conscious mice after intravenous bolus administration.



Blood levels of unchanged **7** after i.v. bolus administration. Shown are means (n = 3). The grey line represents the terminal elimination phase of the compound (non compartmental analysis, t= 2, 4, 8 h). Lower limit of quantification (LLOQ) was 0.7 nM.

Figure S8: Pharmacokinetic profile of **7** in conscious mice after oral administration.



Blood levels of unchanged **7** after oral administration to conscious mice. Shown are means \pm standard error of the mean (n = 3).

6 FGFR4 mass spectroscopy studies

Mass spectrometry determination of covalent adduct formation:

20-30 μM of dephosphorylated human FGFR4 (442-753) wild type, C552A variant, or C477A variant, was prepared prior to MS by passing an aliquot over a NAP-5 column (17-0853-01, GE Healthcare) to remove glycerol. Fractions consisting of 100 μL aliquots were collected using Low-Bind protein eppendorf tubes on ice (Z666491 Sigma). The elution buffer was composed of 50 mM Tris pH 8.0; 150 mM NaCl; 1 mM EDTA (reagents were purchased from Sigma). The fractions were quantified using the Nanodrop Instrument by Witec. Each reaction was incubated with compound for 2 h at RT in a 10 μL sample containing 2-4 μg of total protein, with a final DMSO content of 5% (SERVA 20835). The compound concentrations were set at 0 μM to 200 μM using a 1 to 2 dilution factor. A Waters LCT Premier XE mass spectrometer coupled with an Agilent 1100 HPLC was used for quantification with the following conditions:

Scans in function: 446

Cycle time (secs): 2.010

Scan duration (secs): 2.00

Interscan delay (secs): 0.01

Retention window (mins): 0.000 to 15.000

Ionization mode: ES+

Data type: Accurate Mass

Function type: TOF MS

Column: Acquity BH300 C4 2.1 x 50 mm, 1.7 μm

Gradient Separation: Using Water /0.05% TFA and Acetonitrile/ 0.04%TFA

Table S6. HPLC gradient profile.

Time	%A	%B	%C	%D	Flow (ml/min)	Pressure
0	80	20	0	0	0.080	200
9.0	0	100	0	0	0.080	200
10.0	0	100	0	0	0.080	200
10.5	80	20	0	0	0.080	200

Identification of the sites on FGFR4 modified by compound 8:

Compound **8**-FGFR4 complex was generated by incubating 1 nmol of FGFR4 with 10 nmol **8** in 20 mM Tris, 150 mM NaCl, 5% glycerol, 1 mM EDTA, 3 mM TCEP, pH 8.0 at room temperature for 15 minutes.

Covalent binding of **8** to FGFR4 was assessed by LC-MS (Agilent 1100 LC coupled to Waters LCT MS) employing a 1 mm x 150 mm (Dr. Maisch, Ammerbuch-Entringen, Germany) column packed with Poros R1/H. The column was kept at 80 °C. A gradient from 20% B to 90% B was run over 20 minutes. The flow rate was 80 µl/min (eluent A: water with 0.05% trifluoroacetic acid, eluent B: 90% acetonitrile with 0.05% trifluoroacetic acid). MS spectra were acquired over a mass range of 500-2000 m/z with a scan time of 0.5 s and data processed using MassLynx software (Waters, Milford, MA).

The intact protein complex analysis confirmed the presence of a single covalent adduct of **8** with the FGFR4 protein.

For the analysis of tryptic peptides of FGFR4, the native FGFR4 and the formed **8**-FGFR4 complex were desalted using HPLC (Agilent 1100) in order to remove excess of ligand. Separation was achieved using a Poros R1/H 2.1 mm x 100 mm (Dr. Maisch, Ammerbuch-Entringen, Germany). The column was kept at 80 °C and flow was 200 µl/min. A gradient from 20% B to 90% B was run in 20 minutes (eluent A: water with 0.1% trifluoroacetic acid, eluent B: 90% acetonitrile with 0.1% trifluoroacetic acid). Peaks corresponding to the modified and unmodified protein were collected and dried under an argon stream. Fractions were suspended in 10 µl 8M urea, 0.3M NH₄HCO₃ pH8.0, incubated with 1 µl 1M dithiothreitol (reduction) at 56 °C for 30 minutes, and finally incubated with 1 µl of 1M iodoacetamide (alkylation) in the dark, at room temperature for 30 minutes. Samples were diluted with water to achieve a final urea concentration of 0.8M. The pH was adjusted to pH8.0 with 1 µl 1M Tris pH10. Finally, trypsin (Promega V5111) was added (protein:enzyme ratio 1:20) and the samples were incubated overnight at 37 °C. Tryptic peptides from native FGFR4 and **8**-FGFR4 complex were analyzed by LC-MS/MS using a UPLC interfaced to a Waters Synapt mass spectrometer (Waters, Milford, MA). The chromatographic separation was carried out on a C₁₈ reversed-phase column (Acquity UPLC BEH C18, 1 x 50 mm, Waters) at a flow rate of 0.12 ml/min. Column was kept at 40 °C and a chromatographic gradient from 0 to 40% B was run in 60 minutes (eluent A: water with 0.1% formic acid, eluent B: acetonitrile with 0.1% formic acid). MS and MS^E spectra were acquired over a mass range of 500-2000 m/z with a scan time of 0.5 s.

Peptides covalently modified with **8** were identified by comparing the peptide maps from native FGFR4 and **8**-FGFR4 complex, respectively. The specific **8** fragment 248.15 m/z, generated in MS^E was used to identify modified peptides in the ESI-LC-MSMS analysis (Fig. S9). The tryptic peptide containing the free P-loop cysteine Cys477 of FGFR4 was only detected in samples derived from the native FGFR4 protein. The peptide containing the modified cysteine Cys477 in the P-loop (main site) and the peptide containing a modified cysteine on residue Cys552 in the middle-hinge region were detected in the sample derived from **8**-FGFR4 complex, Figures S10 and S11.

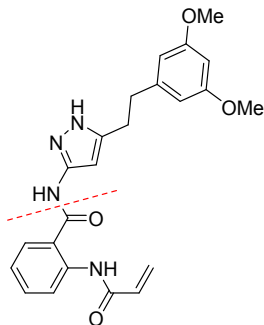
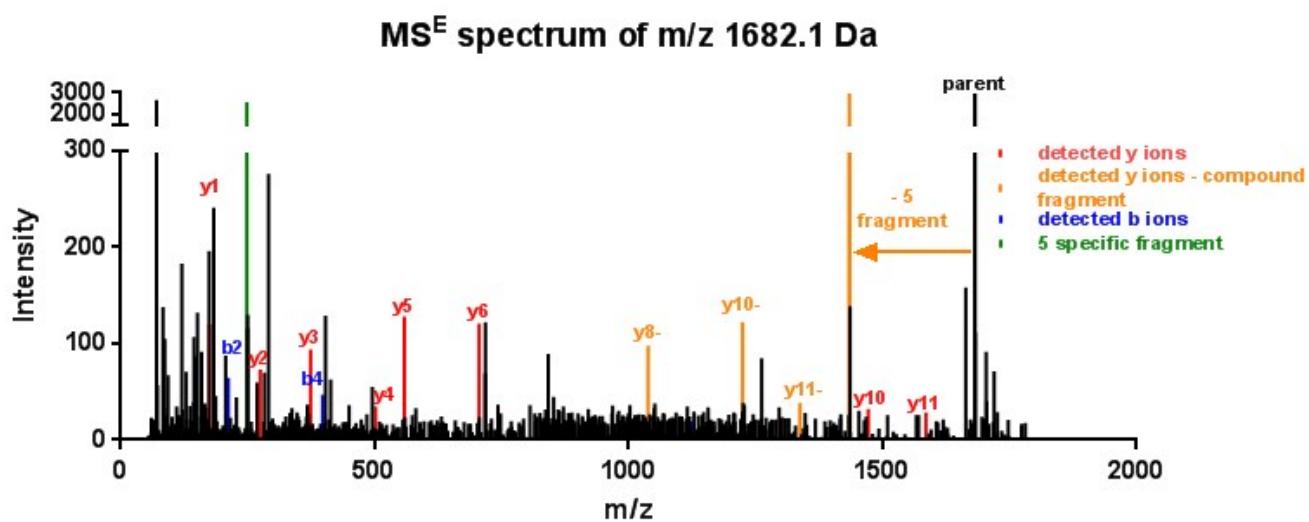


Figure S9. Fragmentation of **8** to give the specific fragment of m/z 248.15

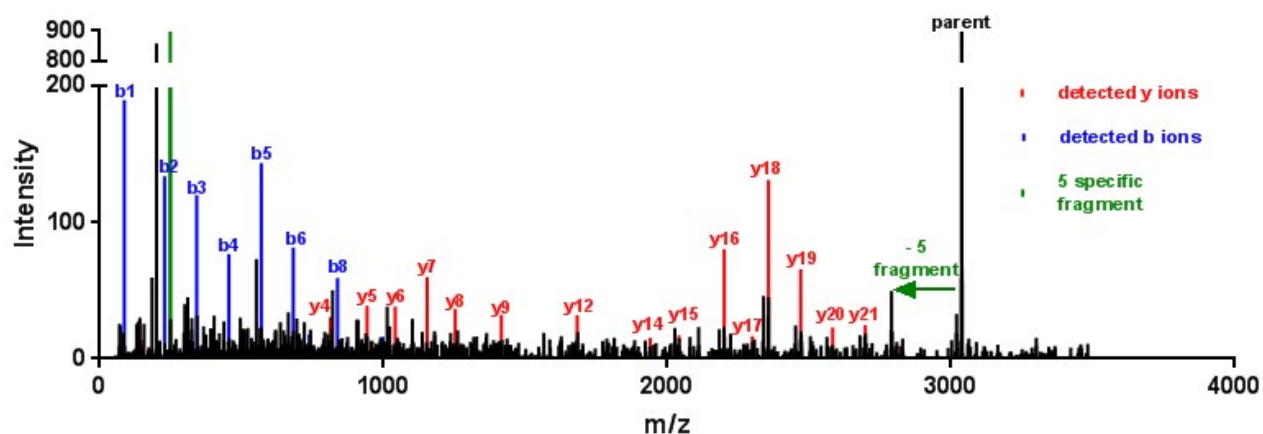


Residue	b	Seq.	y	Residue
1		P	1682.11	12
2	211.14	L	1585.05	11
3	268.17	G	1471.97	10
4	397.21	E	1414.95	9
5	454.23	G	1285.9	8
6	977.71	C + 8	1228.88	7
7	1124.78	F	705.4	6
8	1181.8	G	558.34	5
9	1309.86	Q	501.31	4
10	1408.93	V	373.26	3
11	1507.99	V	274.19	2
12		R	175.12	1

Theoretical b and y ions

Figure S10. MS^E of modified peptide containing P-loop cysteine-477.

MS^E spectrum of m/z 3037.8 Da



Residue	b	Seq.	y	Residue
1		N	3037.84	24
2	228.13	I	2923.8	23
3	341.22	I	2810.72	22
4	455.26	N	2697.63	21
5	568.35	L	2583.59	20
6	681.43	L	2470.5	19
7	738.45	G	2357.42	18
8	837.52	V	2300.4	17
9	997.55	C carbamidomethylated	2201.33	16
10	1098.6	T	2041.3	15
11	1226.66	Q	1940.25	14
12	1355.7	E	1812.19	13
13	1412.72	G	1683.15	12
14	1509.77	P	1626.13	11
15	1622.86	L	1529.08	10
16	1785.92	Y	1415.99	9
17	1884.99	V	1252.93	8
18	1998.07	I	1153.86	7
19	2097.14	V	1040.78	6
20	2226.18	E	941.71	5
21	2749.66	C + 8	812.67	4
22	2820.7	A	289.19	3
23	2891.74	A	218.15	2
24		K	147.11	1

Theoretical b and y ions

Figure S11. MS^E of modified peptide containing hinge region cysteine-552.

7 FGFR4 X-ray structure determinations

FGFR4 purification: The crystal structure of **8** in complex with FGFR4 was obtained with an FGFR4 construct comprising residues from 449 to 753 (Uniprot P22455) with a K506A mutation and with an *N*-terminal 6XHis tag followed by a PreScission cleavage site. The crystal structure of **9** in complex with FGFR4 was obtained with an FGFR4 construct comprising residues from 449 to 753 with an *N*-terminal 6XHis tag followed by a PreScission cleavage site. The purification of both modified FGFR4 constructs were carried out in the same way. Briefly FGFR4 expressed intracellularly in Sf9 cells was homogenized by Frenchpress and first purified by NiNTA affinity chromatography. Following Precision and phosphatase treatment at 4 °C for 18 h, protein was further purified by Mono-Q chromatography, and finally polished by Superdex75 gel filtration chromatography.

Crystallization: Purified FGFR4 protein in buffer (20 mM TRIS, 150 mM NaCl, 3M TCEP, 1 mM EDTA, pH8.0) was mixed with **8** or **9** in excess and concentrated to 5.8 mg/ml and 10 mg/ml, respectively, and was set up for crystallization with method of vapor diffusion by 1:1 mixing with reservoir solution in a total size of 0.4 ul at 294 K. The initial crystals, which typically did not diffract well, were crushed and used for matrix seeding. The well-diffracting crystals for **8** in complex with FGFR4 were obtained in condition containing 0.2M Lithium Sulfate monohydrate, 0.1M Bis-Tris and 25% PEG3350, while the well-diffracting crystals for **9** were obtained in condition containing 0.2M Lithium Sulfate and 25% PEG3350. 10% glycerol was used as cryo-protectant for both complex crystals which were directly flash cooled in liquid nitrogen for data collection.

Structure determination: Diffraction data for both complex crystals were collected at Swiss Light Source (Villigen, Switzerland) at the beam of PXII with a Pilatus pixel detector using x-ray radiation wavelength of 1 Å. The collected data were processed by XDS and XSCALE and the structure was resolved with molecular replacement method with the program PHASER by using an internal unpublished Apo FGFR4 as search model. Iterative model building and refinement were performed with the programs Coot and AUTOBUSTER. Key parameters are included in Table S7.

The structures are deposited with the Worldwide Protein Data Bank:

8: Fibroblast growth factor receptor 4 kinase domain (449-753) in complex with the irreversible ligand NVP-CMN813. PDB ID: 5NWZ.

9: Fibroblast growth factor receptor 4 kinase domain (449-753) in complex with the irreversible ligand CGA159527. PDB ID: 5NUD.

Table S7. Parameters for the cocrystal structures of **8** and **9** with FGFR4.

	8	9
Data collection		
Space group	P21 21 21	C2 2 21
Cell dimensions		
<i>a, b, c</i> (Å)	47.398, 75.958, 181.052	82.899, 87.0554, 182.052
α, β, γ (°)	90, 90, 90	90, 90, 90
Resolution (Å)	2.37-47.25	2.5-27.88
R_{merge}	16%	18%
$I / \sigma I$	13.66	8.67
Completeness (%)	99.9	99.9
Redundancy	6.52	6.52
Refinement		
Resolution (Å)	2.37-47.25	2.5-27.88
No. reflections	23734	23160
$R_{\text{work}} / R_{\text{free}}$	21.45/24.1%	21.86%/25.43%
R.m.s. deviations		
Bond lengths (Å)	0.01	0.01
Bond angles (°)	1.12	1.19

8 Determination of the FGFR4 resynthesis rates

For pulsed SILAC experiments (see reference 30 in the main text), cells were transferred to culture medium in which Lysine and Arginine have been replaced by their 'heavy' counterparts (L-Lysine:2HCl $^{13}\text{C}_6$ and L-Arginine:HCl $^{13}\text{C}_6$, $^{15}\text{N}_4$, Cambridge Isotope labs CLM-2247 and CNLM-539, respectively). After exposure to the heavy amino acids, cells were lysed in M-PER lysis buffer (ThermoFisher #87787) supplemented with Complete Protease Inhibitor Cocktail (Roche #11836145001), PhosSTOP (Roche #04906837001) and 1mM PMSF (Sigma #P7626). Subsequently, FGFR4 was partially purified by immunoprecipitation using the monoclonal antibody MAB#685 (R&D Systems). Immuno-precipitated proteins were eluted by heating in LDS sample buffer (Invitrogen) and separated by SDS-PAGE. Four gel slices, roughly corresponding to the molecular weight range between 75 and 150 kDa were excised from each gel lane and digested with trypsin. Tryptic peptides were analyzed by liquid chromatography coupled to electrospray tandem mass spectrometry (LC-MSMS) on an LTQ Orbitrap XL and an Eksigent nano2D system equipped with a home-made 150 mm x 75 μ column packed with Magic AQ (3 μ , 200A) particles. Peptides were identified using a top 8 method in which each full MS scan in the Orbitrap was followed by 8 ion trap MSMS scans of the most intense precursors using collision-induced dissociation. Data analysis was performed with MaxQuant v1.0.13.13,⁵⁹ using the IPI human protein database (v3.87). Peptides from FGFR4 could be detected in the middle 2 of the 4 gel bands. Protein turnover was estimated by averaging the heavy/light log₂ratios of the individual peptides as provided by MaxQuant, excluding modified and miscleaved peptides. Because in HUH7 cells a mixture of two FGFR4 isoforms was present (see results section below), only the measurements in the upper of the two bands, enriched in the full-length membrane-bound isoform 1 (Uniprot P22455-1) were taken into account. For the purpose of this analysis 'half-life' is defined as the time-point at which the cells have equal levels of heavy and light proteins.

Results: The apparent turnover rate of the FGFR4 protein was measured by incorporating stable isotope labeled Lysine and Arginine, the so-called pulsed SILAC method. In a first pulsed SILAC experiment with the HUH7 cells covering a wide time-course of 4 h to 48 h, it became evident that FGFR4 was synthesized rapidly, reaching a heavy/light (H/L) ratio of >3 already after 4 h (Log₂ratio H/L = 1.8 ± 0.3 , n=20). Therefore in a next experiment, we narrowed down the time-window, measuring H/L ratios after 1, 2, and 4 h. Consistent with the previous measurement, we estimated that the half-life of FGFR4 in HUH7 cells is close to 1 h (see Fig. S12). An accurate determination is challenging because HUH7 cells contain a mixture of similar amounts of two isoforms of FGFR4 (isoforms 1 and 2, UniProt P22455-1 and P22455-2, respectively). These are partially separated in the SDS-PAGE gel, the majority of the larger isoform 1 ending up in the higher molecular weight band and the opposite for the smaller isoform 2. Based on the measurement of the few peptides unique to each of these isoforms, see Figure S13, the membrane-bound isoform 1 turns over with a half-life of less than 1 hr, but isoform 2 has a longer half-life in the range of 8 or more hours, Figure S13. In contrast, in Hep3B cells the major isoform appears to be isoform 1, which turns over with a slightly lower rate than in HUH7 cells resulting in a H/L ratio of 2.8 after 4h (Log₂ratio H/L 1.5 ± 0.3 , n=20), corresponding to a half-life of between 1 and 2 h.

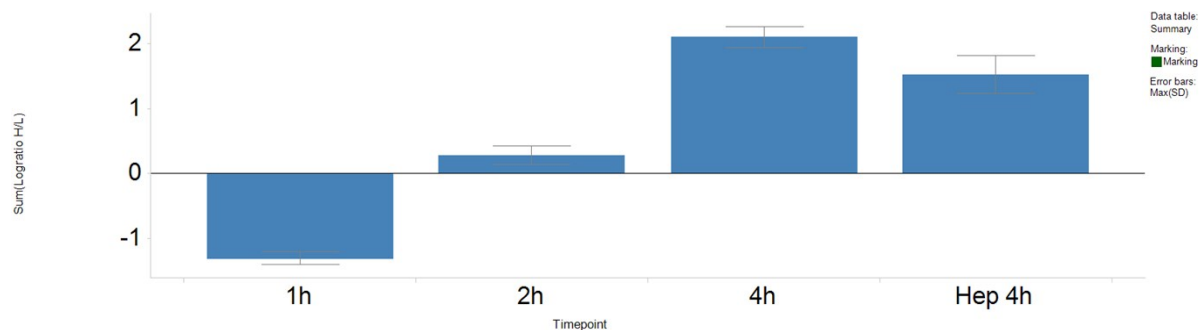


Figure S12. Turnover of FGFR1 in HUH7 and Hep3B cells. Bars represent average H/L log₂ratio over all unmodified and fully tryptic peptides as detected in the gel band most enriched in FGFR4 isoform 1. In all samples one peptide (QFSLESGSSGK) was detected that is not shared between isoforms 1 and 2, showing significantly higher H/L ratios (log₂ratio of 0.8 at 1 h and 3.6 at 4 h). This suggests that the graph underestimates the actual turnover. Three unique peptides for isoform 2 ([TK]SPTLQFSLESGSSGK and IPHLTCDLTPAGR) were not consistently detected in all samples, but their H/L ratios suggest a half-life for isoform 2 of 8 h or more (H/L log₂ratio of -2.5 at 2 h, n=4).

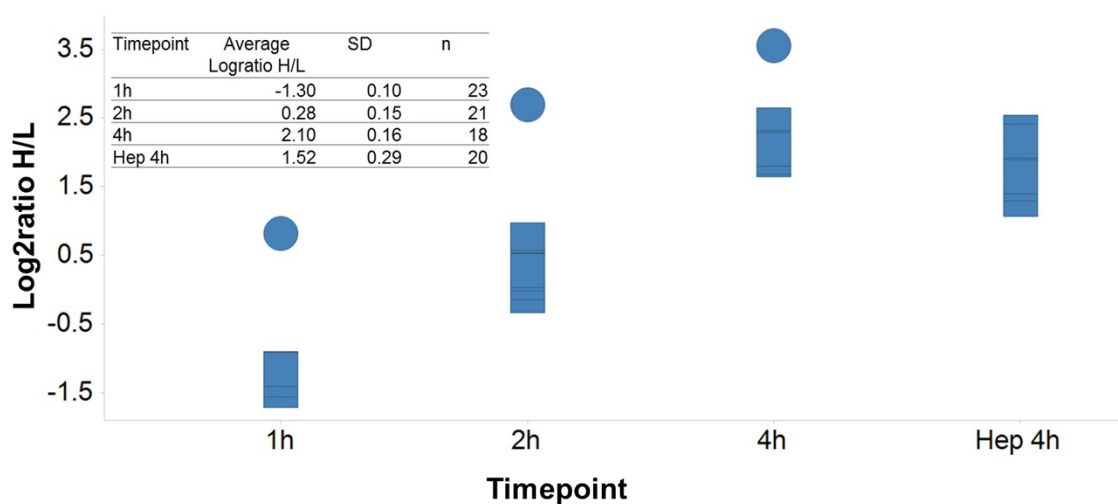


Figure S13. Turnover of FGFR1 in HUH7 and Hep3B cells

Squares represent log₂ratios H/L for all unmodified and fully tryptic peptides as detected in the gel band most enriched in FGFR4 isoform 1 (see text). Circles indicate the one detected peptide in HUH7 cells (QFSLESGSSGK) that is not shared between isoforms 1 and 2. This peptide shows significantly higher H/L ratios (log₂ratio of 0.8 at 1 h and 3.6 at 4 h), suggesting that the graph underestimates the actual turnover. Three unique peptides for isoform 2 ([TK]SPTLQFSLESGSSGK and IPHLTCDLTPAGR) were not consistently detected in all samples (not shown), but their H/L ratios suggest a half-life for isoform 2 of 8 h or more (H/L log₂ratio of -2.5 at 2 h, n=4).

9 Compound 10 X-ray structure determination

The crystal data for compound **10** have been deposited with the Cambridge Crystallographic Data Centre, CIF: 1546562.

Supplementary information references

- 1 Allwein, S. P.; Roemmele, R. C.; Haley, Jr., J. J.; Mowrey, R. D.; Petrillo, D. E.; Reif, J. J.; Gingrich, D. E.; Bakale, R. P. Development and scale-up of an optimised route to the ALK inhibitor CEP28122. *Org. Process Res. Dev.* **2012**, *16*, 148-155.
- 2 Rainer, A.; Andersen, E.; Christen, M.; Hagenbach, A.; Heusser, C.; Papegiorgiou, C.; Schreier, M. H.; Wienand, A. Preparation of quinolinecarboxamides and indolecarboxamides as DHODH blocking B cell inhibitors. WO 1999/041239, August 19th 1999.
- 3 Papageorgiou, C.; von Matt, A.; Joergensen, J.; Andersen, E.; Wagner, K.; Beerli, C.; Than, T.; Borer, X.; Florineth, A.; Rihs, G.; Schreier, M. H.; Weckbecker, G.; Heusser, C. Aromatic quinolinecarboxamides as selective, orally active antibody production inhibitors for prevention of acute xenograft rejection. *J. Med. Chem.* **2001**, *44*, 1986-1992.
- 4 Bairoch, A.; Boeckmann, B. The SWISS-PROT protein sequence data bank: current status. *Nucleic Acids Res.* **1994**, *22*, 3578-3580.
- 5 Notredame, C.; Higgins, D., G.; Heringa, J. T-Coffee: A novel method for fast and accurate multiple sequence alignment. *J. Mol. Biol.* **2000**, *302*, 205-217.
- 6 Vriend, G. WHAT IF: A molecular modeling and drug design program. *J. Mol. Graph.* **1990**, *8*, 52-56.
- 7 Mohamadi, F.; Richards, N. G. J.; Guida, W. C.; Liskamp, R.; Lipton, M.; Caufield, C.; Chang, G.; Hendrickson, T.; Still, W. C. MacroModel – An integrated software system for modeling organic and bioorganic molecules using molecular mechanics. *J. Comput. Chem.* **1990**, *11*, 440.
- 8 Warmuth, M.; Kim, S.; Gu, X.; Xia, G.; Adrián, F. Ba/F3 cells and their use in kinase drug discovery. *Curr. Opin. Onc.* **2007**, *19*, 55.
- 9 Cox, J.; Mann, M. MaxQuant enables high peptide identification rates, individualized p.p.b.-range mass accuracies and proteome-wide protein quantification. *Nat. Biotechnol.* **2008**, *26*, 1367-1372.